Agung et al. *Zool. Res.* 2022, 43(5): 767−786
https://doi.org/10.24272/j.issn.2095-8137.2022.105

ZR | Zoological Research

Article Open Access

Description of two new species of *Hemiphyllodactylus* (Reptilia: Gekkonidae) from karst landscapes in Yunnan, China, highlights complex conservation needs

Ade Prasetyo Agung[1,2,*], Ada Chornelia[1,2], L. Lee Grismer[3], Jesse L. Grismer[3], Evan S. H. Quah[4,5], Jian-Mei Lu[1,2], Kyle W. Tomlinson[6], Alice C. Hughes[1,7,*]

[1] *Landscape Ecology Group*, *Center for Integrative Conservation*, *Xishuangbanna Tropical Botanical Garden*, *Chinese Academy of Sciences*, *Menglun*, *Mengla*, *Yunnan* 666303, *China*

[2] *University of Chinese Academy of Sciences*, *Beijing* 101408, *China*

[3] *Herpetology Laboratory*, *Department of Biology*, *La Sierra University*, *Riverside*, *California* 92515, *USA*

[4] *Institute for Tropical Biology and Conservation*, *Universiti Malaysia Sabah*, *Jalan UMS*, *Kota Kinabalu*, *Sabah* 88400, *Malaysia*

[5] *Lee Kong Chian Natural History Museum*, *National University of Singapore*, *Singapore* 117377, *Singapore*

[6] *Community Ecology and Conservation Group*, *Center for Integrative Conservation*, *Xishuangbanna Tropical Botanical Garden*, *Chinese Academy of Sciences*, *Menglun*, *Mengla*, *Yunnan* 666303, *China*

[7] *School of Biological Sciences*, *University of Hong Kong*, *Pokfulam*, *Hong Kong SAR*, *China*

ABSTRACT

Karst habitats are hotspots of diversity and endemism. Their naturally fragmented distributions across broad geographic landscapes have led to the complex array of smaller evolutionary ecosystems that present unique challenges from a conservation perspective. Comprehensive biodiversity assessments of karst habitats have revealed that these ecosystems contain an almost unparalleled level of endemism, and many site-restricted species remain undescribed, thus posing considerable challenges for effective conservation management. Small rock-dwelling species, such as geckos, may be particularly prone to such isolation. In this paper, we discuss one such genus, i.e., *Hemiphyllodactylus*, and explore its diversity across karst landforms in Yunnan Province, southwestern China. Based on morphological and genetic data, we describe two new species of *Hemiphyllodactylus* from karst habitats in Simao District and Yanshan County. A phylogenetic tree for *Hemiphyllodactylus* was constructed using 1 039 base pairs (bp) of the mitochondrial NADH dehydrogenase subunit 2 gene (*ND2*). The Simao and Yanshan specimens can be distinguished from all other congeners within their respective subclades based on uncorrected genetic pairwise distances greater than 6.3% and 4.3% respectively, as well as significant morphological differences. The discovery and description of these

Received: 13 June 2022; Accepted: 11 August 2022; Online: 12 August 2022

Foundation items: This study was supported by the National Natural Science Foundation of China (U1602265, Mapping Karst Biodiversity in Yunnan), Strategic Priority Research Program of the Chinese Academy of Sciences (CAS) (XDA20050202), High-End Foreign Experts Program of Yunnan Province (Y9YN021B01, Yunnan Bioacoustic Monitoring Program), CAS 135 Program (2017XTBG-T03), and Chinese Academy of Sciences Southeast Asia Biodiversity Research Center Fund (Y4ZK111B01).

*Corresponding authors, E-mail: prasetyo.ade22@gmail.com; ach_conservation2@hotmail.com

two new species brings the total number of described *Hemiphyllodactylus* species in China to 14 and indicates many more undescribed species from unsurveyed karst regions await discovery. Our findings suggest that karst ecosystems in Yunnan support a higher diversity of *Hemiphyllodactylus* than previously known. This study also highlights the importance of karst ecosystems as refugia for site-specific endemic species and the need for heightened conservation efforts.

Keywords: Discovery; Endemism; Geckos; Reptiles; South China

INTRODUCTION

Karst landscapes are characterized by high endemism due to their distinct ecological niches, which allow for the diversification of a wide variety of species (Clements et al., 2006; Grismer et al., 2021). However, these naturally fragmented ecosystems are challenging, as each lone karst formation may host species found nowhere else. Almost every research expedition of karst landforms (both caves and outer rocky surfaces) has uncovered new species with localized distributions (Agung et al., 2021; Dittmar et al., 2005; Huang et al., 2019; Quah et al., 2021; Tian & Huang, 2015), thereby identifying karsts as hotspots of endemism and biodiversity and priorities for conservation. Karst species are also often highly specialized, with poor dispersal capabilities due to their adaptations to the unique abiotic environments of karst ecosystems, such as microclimate, light intensity, and topography (e.g., fissured cliffs) (Whitten, 2009). Thus, understanding the distributions and patterns of endemism and diversity is critical for developing effective conservation plans for the region as many cryptic herptiles may have been overlooked (Vieites et al., 2009).

As the largest family of geckos, Gekkonidae shows high levels of endemism in karst systems. For example, Grismer et al. (2014, 2018b, 2018c, 2020a, 2021) has reported over 100 gecko species endemic to karsts in Southeast Asia, underscoring the need for further work to gain a more complete understanding of the diversity and range of karst-dependent taxa. Given their occurrence in fragmented karst hills and their limited dispersal capabilities, it is likely that more species are waiting to be described. In support of this, Grismer et al. (2018a) identified 12 new gecko species within two weeks in a single study of karsts in Myanmar, with similar patterns likely to exist in karsts across Southeast Asia.

Hemiphyllodactylus Bleeker, 1860 (commonly known as half leaf-fingered geckos, dwarf geckos, or slender geckos), belongs to the family Gekkonidae. Recently, many new species of this genus have been discovered in vegetated karst ecosystems (Do et al., 2020; Grismer et al., 2018b; Nguyen et al., 2020; Zhang et al., 2020), many of which are endemic to single karst hills. However, like other small organisms (e.g., snails, millipedes, and other invertebrates), this genus is often overlooked, and given the highly endemic nature of the group, more targeted protection is clearly needed.

The genus is widely distributed across South Asia, Southeast Asia, South China, and the western Pacific islands (Agarwal et al., 2019; Grismer et al., 2013; Zug, 2010). Generally, *Hemiphyllodactylus* species are small in body size (snout-vent length<63 mm), nocturnal, scansorial, forest-dwelling, and well camouflaged in their environments (Grismer et al., 2013; Zug, 2010), and thus easily overlooked unless specifically targeted. Most members of the genus are confined to tropical and subtropical montane regions in mainland Indochina, although some are also restricted to islands (Agarwal et al., 2019; Eliades et al., 2019; Grismer et al., 2013; Zug, 2010). To date, *Hemiphyllodactylus* consists of two main groups, i.e., *harterti* and *typus*. The *harterti* group is composed of upland species from Peninsular Malaysia, while the *typus* group is comprised of all other species from the entire range of the genus (Grismer et al., 2013). Many of these species are limited to a single site or a limited number of sites, and some “species” are suspected to represent complexes that require further work for accurate species delineation and description. This is especially important given the high rates of karst loss across Southeast Asia and South China, estimated to be 5.7% per year (Hughes, 2017). Thus, without information to ensure the identification of key sites, there is significant potential for species loss (Hughes, 2017).

In recent years, *Hemiphyllodactylus* research and discoveries have experienced a renaissance, with species descriptions increasing every year from 2013. Since then, the number of species has jumped from 14 to 52, mostly from karst regions in Myanmar, Laos, and Vietnam (Uetz et al., 2021). In contrast, gekkonid research in karst regions of South China continues to lag, highlighting the need for in-depth exploration of these areas. This deficiency in field research has resulted in an underestimation of *Hemiphyllodactylus* diversity in China. For example, in Yunnan Province, all populations of *Hemiphyllodactylus* were previously considered to be a single widespread species (*H. yunnanensis*), until integrative taxonomic study revealed multiple species under the nomen *H. yunnanensis* (Grismer et al., 2013).

At present, 12 described species of *Hemiphyllodactylus* are found in South China: i.e., *H. changningensis* Guo, Zhou, Yan & Li, 2015; *H. dupanglingensis* Zhang, Qian & Yang, 2020; *H. dushanensis* Zhou & Liu, 1981; *H. hongkongensis* Sung, Lee, Ng, Zhang & Yang, 2018; *H. huishuiensis* Yan, Lin, Guo, Li & Zhou, 2016; *H. jinpingensis* Zhou & Liu, 1981; *H. longlingensis* Zhou & Liu, 1981; *H. typus* Bleeker, 1860; *H. yunnanensis* Boulenger, 1903; *H. zayuensis* Jiang, Wang, & Che, 2020, *H. zhutangxiangensis* Agung, Grismer, Grismer, Quah, Chornelia, Lu & Hughes, 2021; and *H. zugi* Nguyen, Lehmann, Le Duc, Duong, Bonkowski & Ziegler, 2013.

Based on fieldwork in the karst areas of Yunnan, we identified several potential new species, including the recently described and published species *H. zhutangxiangensis* (Agung et al., 2021). Here, we describe two new species, with our preliminary work also suggesting several other species awaiting description. In the current study, we phylogenetically delimited new evolutionary lineages based on molecular evidence and diagnosed those lineages based on morphological evidence, with descriptions of the new species. We also discuss the relevance of mapping distributions such

as these as a basis for conservation of range-limited, site-endemic species that may be particularly vulnerable to extinction without better inclusion in conservation and environmental impact assessments.

MATERIALS AND METHODS

Field sites and specimen collection

Surveys were conducted in August to September 2018 and June to July 2019 in karst landscapes across Yunnan. Permission to conduct surveys and collect samples was granted by relevant local protected area authorities and ethics approval for research was granted by the Ethics Committee of Xishuangbanna Tropical Botanical Garden, Chinese Academy of Sciences, China. In total, 139 *Hemiphyllodactylus* specimens were collected by hand from 13 different karst areas (Table 1). Specimens were collected at night (between 2000h–2200h) as geckos are nocturnal and actively forage during this time. All *Hemiphyllodactylus* specimens were photographed in the morning after capture to record coloration and patterns. The specimens were euthanized using Tricaine MS-222 solution injected into the intracelomic cavity (Conroy et al., 2009). Tissue samples were obtained from the liver of each individual and stored in 95% ethanol separately for further genetic analysis. The specimens were then preserved in 10% formalin and transferred to 70% ethanol for storage prior to morphological investigation. After investigation, the specimens were deposited in the Kunming Natural History Museum of Zoology, Kunming Institute of Zoology (KIZ), Chinese Academy of Sciences, China. All animal procedures were performed in accordance with the ethical standards of the institution at which the study was conducted (Xishuangbanna Tropical Botanical Garden, Chinese Academy of Sciences).

DNA isolation, sequencing, and phylogenetic analyses

Genomic DNA of the 139 newly collected specimens was isolated from liver tissue following proteinase K DNA extraction protocols using a QIAGEN Genomic-tip 2500 (www.qiagen.com) DNA extraction kit. We amplified the complete mitochondrial NADH dehydrogenase subunit 2 gene (mtDNA-*ND2*), totaling 1 039 bp, using primers L4437b and H5934 following Macey et al. (1997) (5'-AAGCAGT TGGGCCCATACC-3' and 5'-AGRGTGCCAATGTCTTTG TGRTT-3', respectively). The protocol for polymerase chain reaction (PCR) amplifications followed Agung et al. (2021). The PCR processes and sequencing were executed at the South China DNA Barcoding Center.

We constructed a dataset for phylogenetic analyses. We downloaded a total of 209 *ND2* sequences from GenBank, containing 205 sequences of extant *Hemiphyllodactylus* species and four *ND2* sequences of other outgroup taxa (*Gehyra fehlmanni*, *G. mutilata*, *Hemidactylus frenatus* and *Lepidodactylus lugubris*), then added the 139 new sequences to the dataset. All downloaded sequences used in the analyses followed Agung et al. (2021), while the newly published sequences in this study are presented in Supplementary Table S1.

Phylogenetic relationships were analyzed using maximum-likelihood (ML) and Bayesian inference (BI) in IQ-TREE (Nguyen et al., 2015; Trifinopoulos et al., 2016) and MrBayes 3.2.7a (Ronquist et al., 2012) on XSEDE using the CIPRES Science Gateway (Cyberinfrastructure for Phylogenetic Research; Miller et al., 2010), respectively. Prior to ML analysis, the best substitution model (TIM+F+R5) was selected for the non-partitioned dataset based on Bayesian information criterion (BIC) in ModelFinder (Kalyaanamoorthy et al., 2017). The ultrafast bootstrap approximation algorithm (UFBoot) was used with 1 000 bootstrap pseudoreplicates (Hoang et al., 2018), where nodes bearing values ≥95 were considered strongly supported (Minh et al., 2013). For BI analysis, default priors were selected, and two independent Markov Chain Monte Carlo (MCMC) algorithms were applied, with four chains in each (three hot and one cold), 50 million generations sampled every 1 000 generations, and the first 25% of samples discarded. All parameters from the two runs were checked in Tracer v1.7.1 (Rambaut et al., 2018), confirming convergences and effective sample sizes (ESS) were >200. Post burn-in sampled trees from both runs were combined and a 50% majority-rule consensus tree was produced. Nodes bearing Bayesian posterior probabilities (BPP) ≥0.95 were considered strongly supported (Huelsenbeck et al., 2001; Wilcox et al., 2002). Uncorrected

Table 1 Location of the 13 selected karst field sites in Yunnan, China

No. point	Location (individuals collected)	Longitude (°)	Latitude (°)	Altitude (m, a.s.l.)
1	Mengyuan town, Mengla County (1)	101.385	21.720	711
2	Simao District, Pu'er City (4)	100.712	22.607	1 273
3	Simao District, Pu'er City (8)	100.803	22.735	1 129
4	Ning'er County, Pu'er City (14)	101.019	23.083	1 436
5	Yongde County (25)	99.232	23.962	1 488
6	Shijiancao, Yimen County (23)	102.163	24.617	1 631
7	Luxi County (2)	103.585	24.474	1 624
8	Luxi County (10)	103.689	24.485	1 824
9	Yanshan County (13)	104.417	23.617	1 536
10	Lishan village, Tong Hai County (11)	102.758	24.072	1 822
11	Qinglong town, Jian Shui County (16)	102.775	23.566	1 333
12	Ka Fang town, Gejiu City (11)	103.144	23.195	1 394
13	Xianren Dong cave, Gejiu City (1)	103.141	23.358	1 801

pairwise distances among and within species were computed using MEGA 7 (Kumar et al., 2016).

Morphological measurements and analyses

We measured mensural and meristic traits of the 139 collected specimens following Zug (2010) and Grismer et al. (2013), with slight modifications following Agung et al. (2021). Mitutoyo Absolute Series-500 digital calipers (accuracy 0.01 mm) were used to measure mensural traits under a dissecting microscope (Nikon SMZ 445), on the left side of the body when possible. Recorded traits included: snout-vent length (SVL), trunk length (TL), head length (HL), head width (HW), eye diameter (ED), snout-eye length (SnEye), naris-eye length (NarEye), and snout width (SnW). Recorded meristic traits included: circumnasal scales (CN), internasal scales (IS), supralabial scales (SL), infralabial scales (IL), chin scales (Chin), ventral scales (VS), dorsal scales (DS), subdigital lamellae wider than long on first finger (SL1F) and toe (SL1T), subdigital lamellae formula determined as number of U-shaped digital pads on digits II–V of hands and feet, number of femoroprecloacal pores, and number of cloacal spurs (CloacS) on each side of hemipenial swelling. We also noted coloration and pattern on the dorsum, presence or absence of dark postorbital stripes extending at least to neck, presence or absence of dorsolateral and ventrolateral stripes, and presence or absence of anteriorly projecting arms of postsacral markings.

We compared the morphology of each new lineage recovered from phylogenetic analysis against published morphological data for selected closely related species to establish significant differences between any of the measured traits. Prior to analysis, we corrected for the effects of body size on mensural traits in each new lineage combined with data from closely related species using the following equation:

$$X\text{adj} = X - \beta(\text{SVL} - \text{SVLmean}) \quad (1)$$

where *X*adj is the adjusted value; *X* is the measured value; β is the unstandardized regression coefficient for each operational taxonomic unit (OTU); SVL is the measured SVL; and SVLmean is the overall average SVL of all OTUs (Lleonart et al., 2000; Thorpe, 1975, 1983; Turan, 1999).

All morphological analyses were computed in R v.4.0.1 (R Core Team, 2020). Each adjusted mensural trait was checked for equal variances across groups using Levene's test. Traits with equal variances ($P \geq 0.05$) were analyzed using ordinary linear models, while traits with unequal variances ($P \leq 0.05$) were analyzed using generalized linear models with weighted least squares (gls) in the "nlme" package (Pinheiro et al., 2020). Error degrees of freedom (df) were calculated with the Satterthwaite approximation, applying the *emmeans* function in the package "emmeans" (Lenth, 2021), which compares appropriate estimates for uneven group variances. For meristic traits (count data), glm models were used. Quasi-Poisson errors were implemented in the glm models as all traits were under-dispersed when checked with the *dispersiontest* function in the "AER" package (Kleiber & Zeileis, 2008). For both mensural and meristic traits, significant differences were first evaluated with a variance test (analysis of variance (ANOVA) or Chi-square tests), and, if significant, subjected to *post hoc* Tukey's HSD tests for mean comparisons involving three or more groups. We also used non-parametric permutation ANOVA (PERMANOVA) to determine whether the posited species differed from closely related species in multi-trait space using the *adonis* and *pairwise.adonis* functions in the "vegan" package (Oksanen et al., 2020) with 50 000 permutations. Lastly, principal component analysis (PCA) was run to test for group separation along the first two principal components using the *prcomp* function.

Designation of species-level lineages

We used an integrated approach to delineate species-level lineages by consolidating phylogenetic position, genetic divergence, and morphological differences. We used three sequential criteria to designate species-level lineages: First, new lineages not clustered within the named species lineages in phylogenetic topology were marked as potential new species. Second, uncorrected pairwise genetic distances among the new lineages with either known species or other putative species lineages were measured, with a 3.0% difference in mtDNA *ND2* considered minimal to define a potential new species. This cut-off was based on Zhang et al. (2020), who reported a 3.6% sequence divergence between *H. linnwayensis* and *H. ywanganensis* after uncorrected pairwise comparison of the 670 bp (partial) *ND2* gene across numerous species, with these two species known to be morphologically distinct (Grismer et al., 2018c). Third, those lineages showing >3.0% genetic difference from their nearest relatives were examined for morphological distinctiveness from closely related species. If this third criterion was also met, the lineage was considered a confirmed new species. Lineages satisfying all three criteria were described. Individuals not satisfying all criteria may also be distinct species, but further data and specimens are needed for this to be established.

RESULTS

Phylogeny

The ML and BI analyses recovered similar tree topologies with strong nodal support, but with a slight difference in the position of *H. khlonglanensis*, i.e., sister species to clades 3 and 4 in the ML tree, but sister species to clade 4 only in the BI tree. Figure 1 shows the topology of the ML tree, including both nodal support values (UFBoot/BPP). Our inferred ML topology was highly consistent with the topology reported by Grismer et al. (2020b). We named all clades following Grismer et al. (2020b) and renamed the South Myanmar lineage, which consisted of *H. zwegabinensis*, *H. kyaiktiyoensis*, and *H. pinlaungensis*, as clade 8.

All 139 Yunnan karst specimens belonged to the *typus* group and were placed into four clades: i.e., clades 3, 4, 6, and 7 (in bold in Figure 1). All specimens were nested and formed OTUs as follows: 25 specimens were from Yongde County, recovered as *H. changningensis* (clade 3); 47 specimens were from Jian Shui County, Yimen County, and Gejiu City, recovered as *H. jinpingensis* and sister to the newly recovered OTU comprised of 22 specimens from Simao

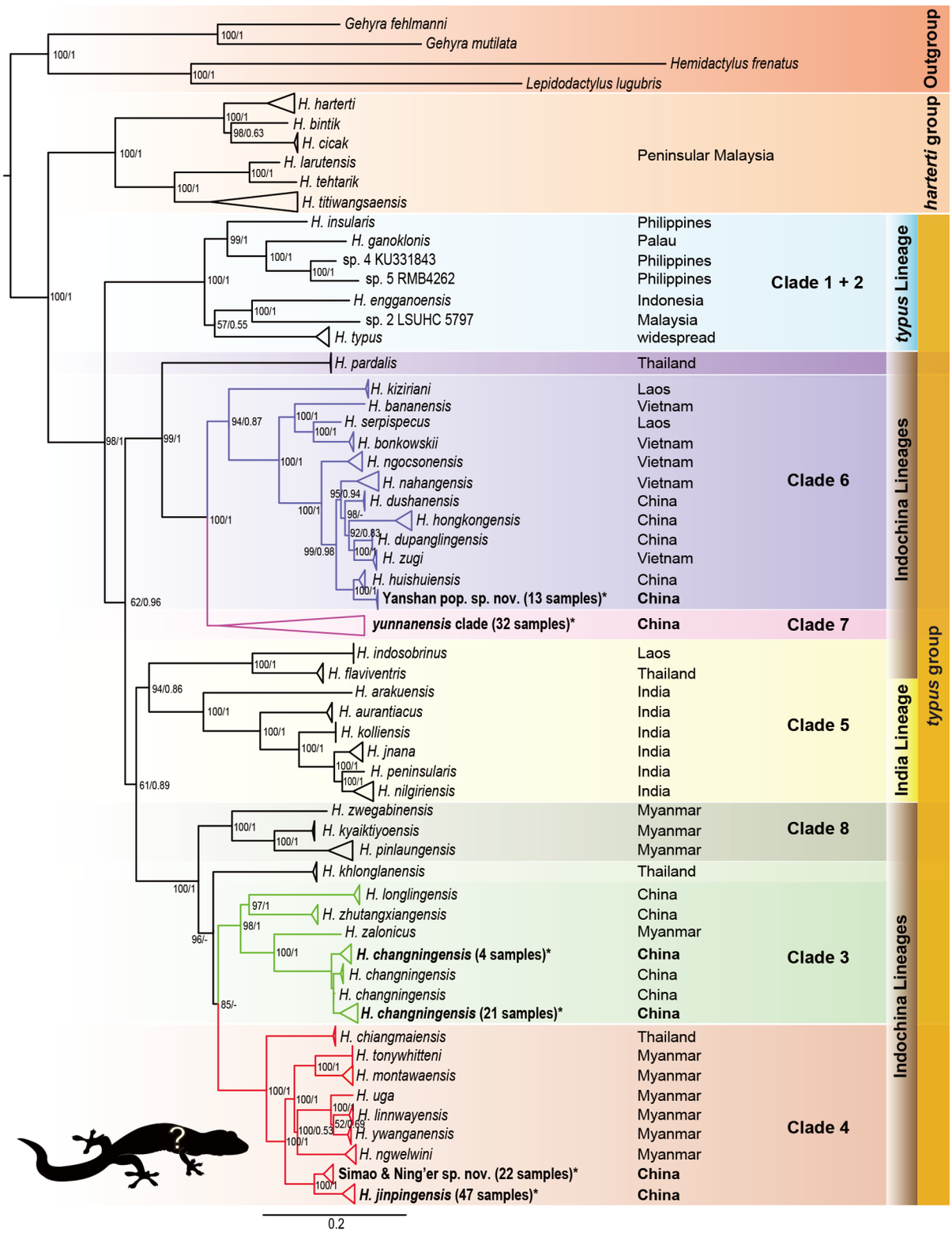

Figure 1 Maximum-likelihood topology illustrating phylogenetic relationships among *Hemiphyllodactylus* species

Nodes shows UFBoot/BPP, respectively. Nodes with ≥95 and 0.95 are highly supported. Asterisk (*) indicates newly collected specimens in this study.

District and Ning'er County (clade 4); 13 specimens were from Yanshan County, recovered as a new OTU (clade 6) and sister to *H. huishuiensis*; and 32 specimens were from multiple locations, including Mengla County, Simao District, Luxi

County, Jianshui County, Gejiu City, and Tonghai County, and nested within the *yunnanensis* clade complex (clade 7). The *yunnanensis* clade (clade 7) consisted of multiple distinct evolutionary lineages, and further analysis is needed to resolve their relationships and taxonomy.

The ML and BI trees recovered two distinct evolutionary lineages in our Yunnan samples, i.e., Simao and Ning'er County population (hereafter referred to as Simao population) in clade 4 and Yanshan County population in clade 6, as described below.

Genetic distance

Uncorrected genetic *P*-distances among and within the *ND2* gene of the newly recovered OTUs (within clades 4 and 6) are presented in Tables 2, 3. The interspecific genetic distances within clade 4 ranged from 2.7% (between *H. ywanganensis* and *H. linnwayensis*) to 14.3% (between *H. chiangmaiensis* and *H. jinpingensis*), and the new Simao population showed at least 6.3% genetic distance to its sister species *H. jinpingensis* (Table 2).

In clade 6, interspecific genetic distances ranged from 4.3% (between new Yanshan population and sister species *H. huishuiensis*) to 23.0% (between *H. kiziriani* and *H. banaensis*; Table 3). The genetic distances of the two new populations (Simao and Yanshan) within their clades (clades 4 and 6, respectively) were above 3%, the threshold used to delineate a new species in this study (see Methods).

Morphological analysis of Simao population

We compared the Simao population to members within clade 4, i.e., *H. jinpingensis*, *H. montawaensis*, *H. ngwelwini*, and *H. tonywhitteni*, as they were the closest relatives to the Simao population containing more than two individuals in each species (*P*-distance=6.3%, 10.2%, 10.5%, and 10.8%, respectively; Table 2). The raw *H. jinpingensis* data used for statistical analysis were obtained from our specimens (45 individuals out of 47 collected from various locations in Yunnan) as no appropriate raw data were available from previous studies. The raw *H. jinpingensis* data are provided in Supplementary Table S2. The raw data for *H. montawaensis* and *H. tonywhitteni* were obtained from Grismer et al. (2018b), and for *H. ngwelwini* were obtained from Grismer et al. (2020a). Linear and general linear model analyses of each morphological trait in the Simao population and its congeners showed that seven mensural traits and eight meristic traits differed significantly among the five groups (Table 4).

Post hoc multiple comparison tests showed significant differences in two mensural and five meristic traits between the *H. jinpingensis* and Simao specimens, although it should be noted that there was overlap in the recorded range of values among individuals across species (see Supplementary Table S3). Of the two mensural traits, *H. jinpingensis* had greater ED, whereas the Simao specimens had greater HW. Furthermore, *H. jinpingensis* had higher values in five meristic traits (VS, SL, IL, SL1F, and SL1T) compared to the Simao

Table 2 Uncorrected genetic *P*-distances (%) in *ND2* (1 039 bp) gene of *Hemiphyllodactylus* in clade 4

No.	Species (*n*)	1	2	3	4	5	6	7	8	9
1	*H. jinpingensis* (51)	**0.6**								
2	*H. montawaensis* (6)	11.9	**0.3**							
3	*H. ngwelwini* (9)	11.8	10.0	**1.2**						
4	*H. linnwayensis* (2)	11.1	10.4	9.4	**0.7**					
5	*H. tonywhitteni* (5)	12.6	5.5	9.7	10.1	**0.0**				
6	*H. ywanganensis* (2)	11.4	9.9	9.0	2.7	8.4	**0.2**			
7	*H. uga* (1)	12.6	10.0	9.9	4.5	9.1	3.4	**–**		
8	*H. chiangmaiensis* (2)	14.3	12.7	13.2	13.9	12.9	13.2	12.7	**0.3**	
9	**Simao pop. (22)**	6.3	10.2	10.5	10.7	10.8	10.8	11.5	12.6	**0.2**

Bold values correspond to average intraspecific distances. *n*: Number of individuals. –: Not available.

Table 3 Uncorrected genetic *P*-distances (%) in *ND2* (1 039 bp) gene of *Hemiphyllodactylus* in clade 6

No	Species (*n*)	1	2	3	4	5	6	7	8	9	10	11	12
1	*H. banaensis* (1)	**–**											
2	*H. bonkowskii* (2)	13.1	**0.7**										
3	*H. dupanglingensis* (3)	16.9	15.4	**0**									
4	*H. dushanensis* (2)	17.5	14.7	5.1	**0.2**								
5	*H. hongkongensis* (4)	16.7	15.4	8.1	7.9	**0.2**							
6	*H. huishuiensis* (5)	15.8	15.4	7.1	6.5	8.7	**0.9**						
7	*H. kiziriani* (3)	23.0	20.6	20.0	20.6	20.2	20.6	**0.3**					
8	*H. nahangensis* (3)	14.9	14.2	5.3	5.4	7.5	6.3	20.3	**1.4**				
9	*H. ngocsonensis* (2)	14.7	14.2	7.5	7.8	10.3	7.7	20.2	7.5	**2.4**			
10	*H. serpispecus* (1)	11.8	8.2	17.2	16.1	17.6	15.5	22.8	15.6	14.2	**–**		
11	*H. zugi* (3)	16.4	15.1	4.9	5.7	7.9	6.9	20.6	6.2	8.2	16.7	**0.3**	
12	**Yanshan pop. (13)**	17.4	16.2	8.6	8.2	9.4	4.3	22.8	8.1	9.3	17.7	9.0	**0.1**

Bold values correspond to average intraspecific distances. *n*: Number of individuals. –: Not available.

Table 4 Summary statistics for each trait of compared species in clade 4

Trait	Levene's test		Regression model	
	Statistic	assignment	Type	*F*-test/*Chi*-square test
Mensural traits				
TrunkL	0.012	Unequal	gls	0.016
ED	0.162	Equal	lm	<0.001
HL	<0.001	Unequal	gls	<0.001
HW	0.002	Unequal	gls	<0.001
NarEye	0.073	Equal	lm	<0.073
SnEye	0.049	Unequal	gls	<0.001
SnW	0.226	Equal	lm	<0.001
Meristic traits				
DS	–	–	glm	<0.001
VS	–	–	glm	<0.001
CN	–	–	glm	0.056
IS	–	–	glm	NS
SL	–	–	glm	<0.001
IL	–	–	glm	<0.001
SL1T	–	–	glm	<0.001
SL1F	–	–	glm	<0.001
CloacS	–	–	glm	NS
Chin	–	–	glm	<0.001

Adjusted mensural traits were tested for normality and did not require transformation. Subsequently, data were subjected to Levene's equality of variance tests and assigned to linear modeling (equal variances) or generalized least squares modeling (unequal variances). Meristic traits were under-dispersed and assessed using glm models with quasi-Poisson error distributions. Variance test probabilities of linear models (*F*-tests) and generalized linear models (*Chi*-square tests) are provided. See Methods for abbreviations. –: Not available. NS: Not significant.

specimens. Two mensural and five meristic traits differed significantly between the *H. montawaensis* and Simao specimens. Of the two mensural traits, *H. montawaensis* had greater HL, whereas Simao specimens had greater HW. Of the five meristic traits, *H. montawaensis* had more VS, but fewer SL, IL, SL1T, and Chin. One mensural and three meristic traits differed significantly between the Simao specimens and *H. ngwelwini*, notably the Simao specimens had shorter HL and fewer VS and Chin, but more IL. Two mensural and seven meristic traits differed significantly between the Simao specimens and *H. tonywhitteni*. Of the two mensural traits, the Simao specimens had a shorter HL, but greater HW. For the meristic traits, the Simao specimens had more CN, SL, IL, SL1F, and Chin, but fewer DS and VS (Figure 2).

Multi-trait spatial analysis using PERMANOVA pairwise comparisons indicated that the five groups (Simao specimens, *H. jinpingensis*, *H. montawaensis*, *H. ngwelwini*, and *H. tonywhitteni*) differed significantly from each other (Table 5). In addition, clustering based on PCA showed that the Simao specimens were morpho-spatially distinct and clustered separately along PC1 with respect to *H. montawaensis* and *H. tonywhitteni*, but partially overlapped with respect to *H. jinpingensis* and *H. ngwelwini*, with 26.7% of the variation loaded most heavily for HL and IL (see Supplementary Table S4 for PCA scores on each trait). For PC2, all groups overlapped with each other, except for *H. montawaensis* and *H. tonywhitteni* (Figure 3). Details on statistical results for group separation along the two axes are presented in Table 6.

Morphological analyses of Yanshan population

We compared the Yanshan population to *H. huishuiensis* (raw data obtained from Yan et al., 2016) and *H. nahangensis* (raw data obtained from Do et al., 2020), as the latter two species were the closest relatives of the Yanshan population based on phylogeny and uncorrected genetic distance (*P*-distance=4.3% and 8.1%, respectively; Table 3). Linear and general linear model analyses of each morphological trait in the Yanshan population and its two closely related species identified significant differences in seven mensural and seven meristic traits (Table 7).

Post hoc multiple comparison tests showed that six mensural and five meristic traits differed significantly between the *H. huishuiensis* and Yanshan specimens, although it should be noted that there was overlap in the recorded range of values among individuals across species (see Supplementary Table S5). Of the six mensural traits, *H. huishuiensis* had greater TrunkL and HL, whereas Yanshan specimens had greater HW, NarEye, SnEye, and SnW. Of the five meristic traits, *H. huishuiensis* had more IS, whereas Yanshan specimens had more CN, CloacS, SL1F, and SL1T. Seven mensural and five meristic traits differed significantly between the Yanshan specimens and *H. nahangensis*. Of the seven mensural traits, Yanshan specimens had greater HW, NarEye, SnEye, and SnW, whereas *H. nahangensis* had greater TrunkL, ED, and HL. Of the five meristic traits, Yanshan specimens had more CN, SL1F, and SL1T, whereas *H. nahangensis* had more DS and IS (Figure 4).

Multi-trait spatial analysis using PERMANOVA pairwise comparison indicated that the three groups (Yanshan

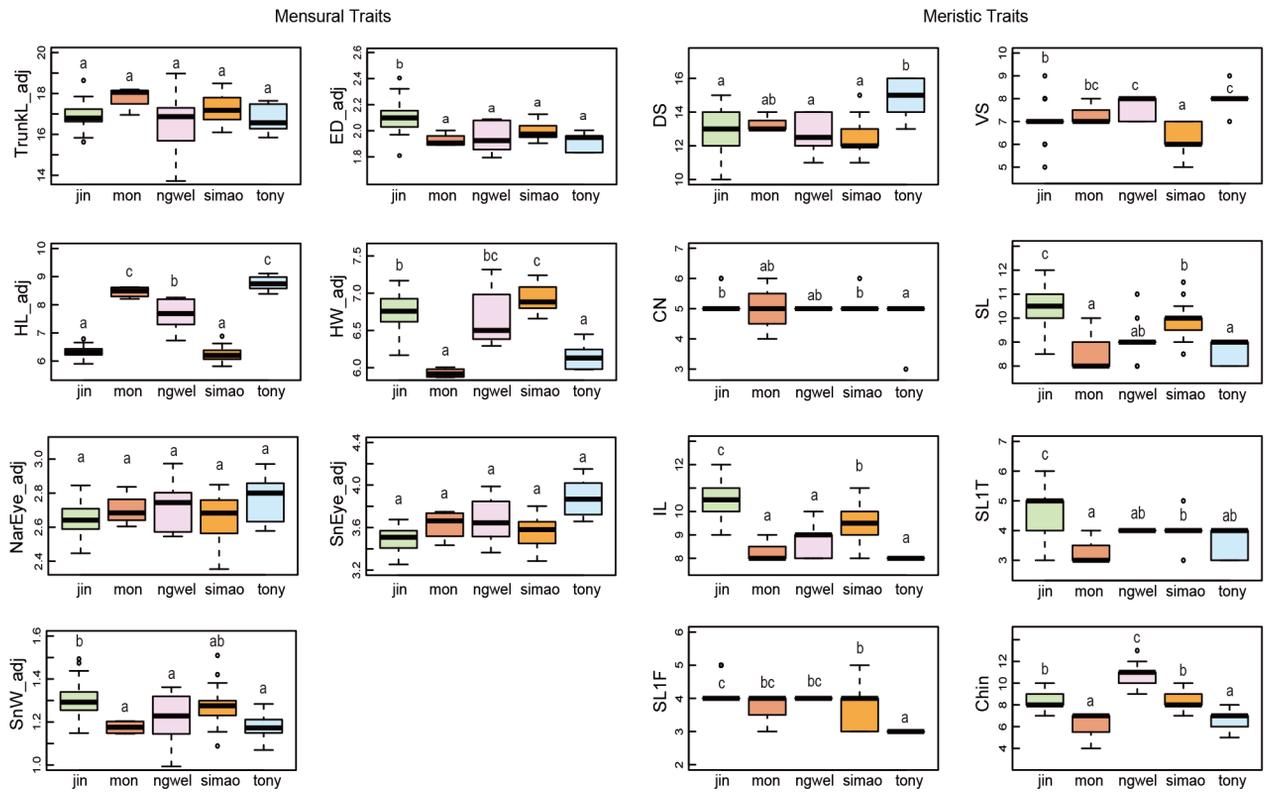

Figure 2 Differences in adjusted mensural (left) and meristic (right) traits between Simao population and closely related species

Mean trait values showing significant differences (P<0.05) are indicated by different letters in each panel. jin: *H. jinpingensis*; mon: *H. montawaensis*; ngwel: *H. ngwelwini*; tony: *H. tonywhitteni*.

Table 5 PERMANOVA pairwise comparisons of multi-trait space of compared species within clade 4

Pairs	F. Model	R2	*P*-value	*P*-adjusted	Sig
simao – jin	13.3	0.174	<0.001	<0.001	***
simao – ngwel	20.5	0.406	<0.001	<0.001	***
simao – tony	28.3	0.531	<0.001	<0.001	***
simao – mon	19.7	0.451	<0.001	<0.001	***
jin – ngwel	26.0	0.338	<0.001	<0.001	***
jin – tony	31.2	0.404	<0.001	<0.001	***
jin – mon	21.4	0.322	<0.001	<0.001	***
ngwel – tony	12.5	0.491	<0.001	0.001	**
ngwel – mon	10.0	0.454	0.001	0.001	**
tony – mon	2.8	0.288	0.024	0.024	*

Sig: Significance levels. *: P<0.05; **: P<0.01; ***: P<0.001 (50 000 permutations). jin: *H. jinpingensis*; ngwel: *H. ngwelwini*; tony: *H. tonywhitteni*; mon: *H. montawaensis*.

population, *H. huishuiensis*, and *H. nahangensis*) differed significantly from each other (Table 8). In addition, clustering based on PCA showed that specimens from Yanshan, *H. huishuiensis*, and *H. nahangensis* were morpho-spatially distinct and clustered separately along PC1, which accounted for 45.7% of variation in the dataset and was loaded most heavily for SL1T, CN, and SnW (see Supplementary Table S6 for PCA scores on each trait). The Yanshan specimens overlapped with *H. huishuiensis* and *H. nahangensis* along PC2, which accounted for 15.5% of variation in the dataset and was loaded most heavily for DS and VS (Figure 5). Details on statistical results for group separation on the two axes are presented in Table 9.

Systematics

Based on phylogenetic evidence, uncorrected genetic distance, and lineage distinction from significantly different morphological characters, the Simao and Yanshan populations likely constitute new evolutionary lineages, and thus represent two new species, as described below.

***Hemiphyllodactylus simaoensis* sp. nov. (Figure 6)**

Suggested English name: Simao slender gecko

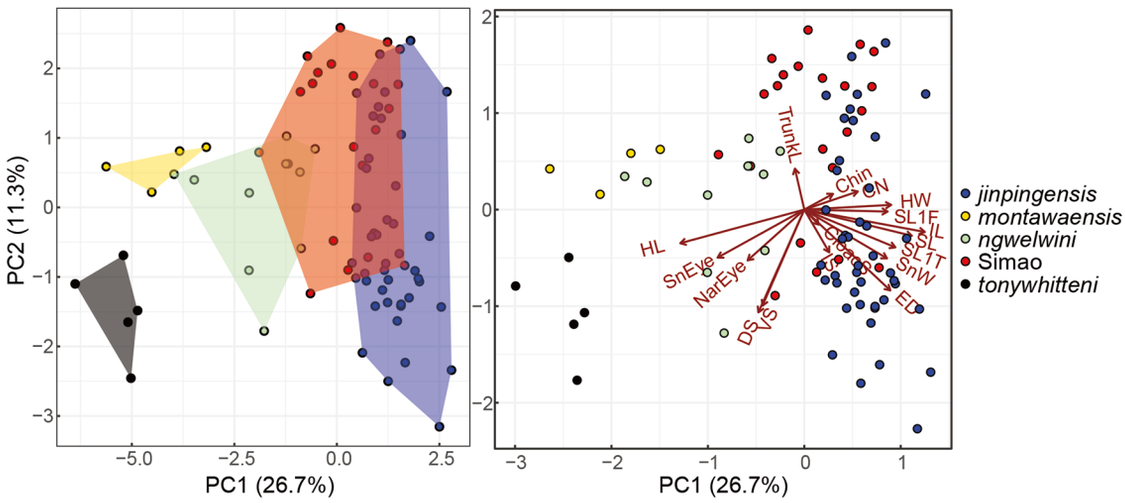

Figure 3 Principal component analysis (left) and biplot (right) of compared species within clade 4

Graphs show morphospatial relationships along first two components. Dots indicate positions of individuals in PCA morphospace and arrows indicate vectors for each morphological trait (acronyms for traits are indicated).

Table 6 Test results for group separation of compared species within clade 4 along first two PCA axes (PC1 and PC2)

PC	Group pairwise	Estimate	*SE*	*df*	t. ratio	*P*-value	Sig
1	jin vs. mon	5.62	0.425	79	13.21	<0.0001	***
	jin vs. ngwel	3.15	0.286	79	11.045	<0.0001	***
	jin vs. simao	1.1	0.213	79	5.16	<0.0001	***
	jin vs. tony	6.64	0.384	79	17.277	<0.0001	***
	mon vs. ngwel	–2.46	0.481	79	–5.118	<0.0001	***
	mon vs. simao	–4.52	0.442	79	10.216	<0.0001	***
	mon vs. tony	1.02	0.546	79	1.875	0.3392	NS
	ngwel vs. simao	–2.05	0.31	79	–6.621	<0.0001	***
	ngwel vs. tony	3.49	0.445	79	7.825	<0.0001	***
	simao vs. tony	5.54	0.403	79	13.747	<0.0001	***
2	jin vs. mon	–1.074	0.627	79	–1.712	0.4324	NS
	jin vs. ngwel	–0.535	0.421	79	–1.27	0.7105	NS
	jin vs. simao	–1.525	0.315	79	–4.847	0.0001	***
	jin vs. tony	1.023	0.567	79	1.804	0.3789	NS
	mon vs. ngwel	0.539	0.71	79	0.76	0.9413	NS
	mon vs. simao	–0.45	0.652	79	–0.691	0.958	NS
	mon vs. tony	2.097	0.805	79	2.605	0.0792	NS
	ngwel vs. simao	–0.99	0.458	79	–2.163	0.2048	NS
	ngwel vs. tony	1.558	0.657	79	2.37	0.1346	NS
	simao vs. tony	2.547	0.595	79	4.284	0.0005	***

PCA scores for each axis were grouped by species and compared pairwise using Tukey HSD tests to adjust for multiple comparisons. Sig: Significance levels. NS: Not significant; ***: *P*<0.001.

Suggested Chinese name: 思茅半叶趾虎

Holotype: Adult male (KIZ 062064) collected on 6 July 2019 by Ade P. Agung, Jian-Mei Lu, and Zong-Bao Yang from forested karst hills in Simao District, Pu'er City, Yunnan Province, China (N22.735°, E100.803°; 1 129 m a.s.l.).

Paratypes: Four adult males (KIZ 062063, KIZ 062066–KIZ 062068) and three adult females (KIZ 062065, KIZ 062069–KIZ 062070), same data as holotype. Five adult males (KIZ 062072, KIZ 062073, KIZ 062077, KIZ 062079, KIZ 062087) and nine adult females (KIZ 062074–KIZ 062076, KIZ 062080–KIZ 062084, KIZ 062088) were collected on 16–17 August 2018 by Ade P. Agung, Ada Chornelia, Jian-Mei Lu, L. Lee Grismer, Jesse L. Grismer, Evan S.H. Quah, Brian Folt, and Myin Kyaw Thura from forested karst in Ning'er County, Pu'er City, Yunnan Province, China (N23.083°, E101.019°; 1 436 m a.s.l.).

Diagnosis: *Hemiphyllodactylus simaoensis* **sp. nov.** can be distinguished from all congeners by a unique combination of the following characters: maximum SVL 40.87 mm; chin scales 7–10; enlarged postmentals; circumnasal scales 5–6;

Table 7 Summary statistics for analysis of each trait of Yanshan population and selected congeners

Trait	Levene's test		Regression model	
	Statistic	Assignment	Type	*F*-test/*Chi* sq test
Mensural traits				
TrunkL	0.029	Unequal	gls	<0.001
ED	0.028	Unequal	gls	0.002
HL	0.093	Equal	lm	<0.001
HW	0.497	Equal	lm	<0.001
NarEye	0.292	Equal	lm	<0.001
SnEye	0.613	Equal	lm	<0.001
SnW	0.311	Equal	lm	<0.001
Meristic traits				
DS	–	–	glm	<0.001
VS	–	–	glm	NS
CN	–	–	glm	<0.001
IS	–	–	glm	<0.001
SL	–	–	glm	0.024
IL	–	–	glm	NS
CloacS	–	–	glm	0.030
SL1F	–	–	glm	<0.001
SL1T	–	–	glm	<0.001
Chin	–	–	glm	NS

Variance test probabilities of linear models (*F*-tests) and generalized linear models (*Chi*-square tests) are provided. –: Not available. NS: Not significant.

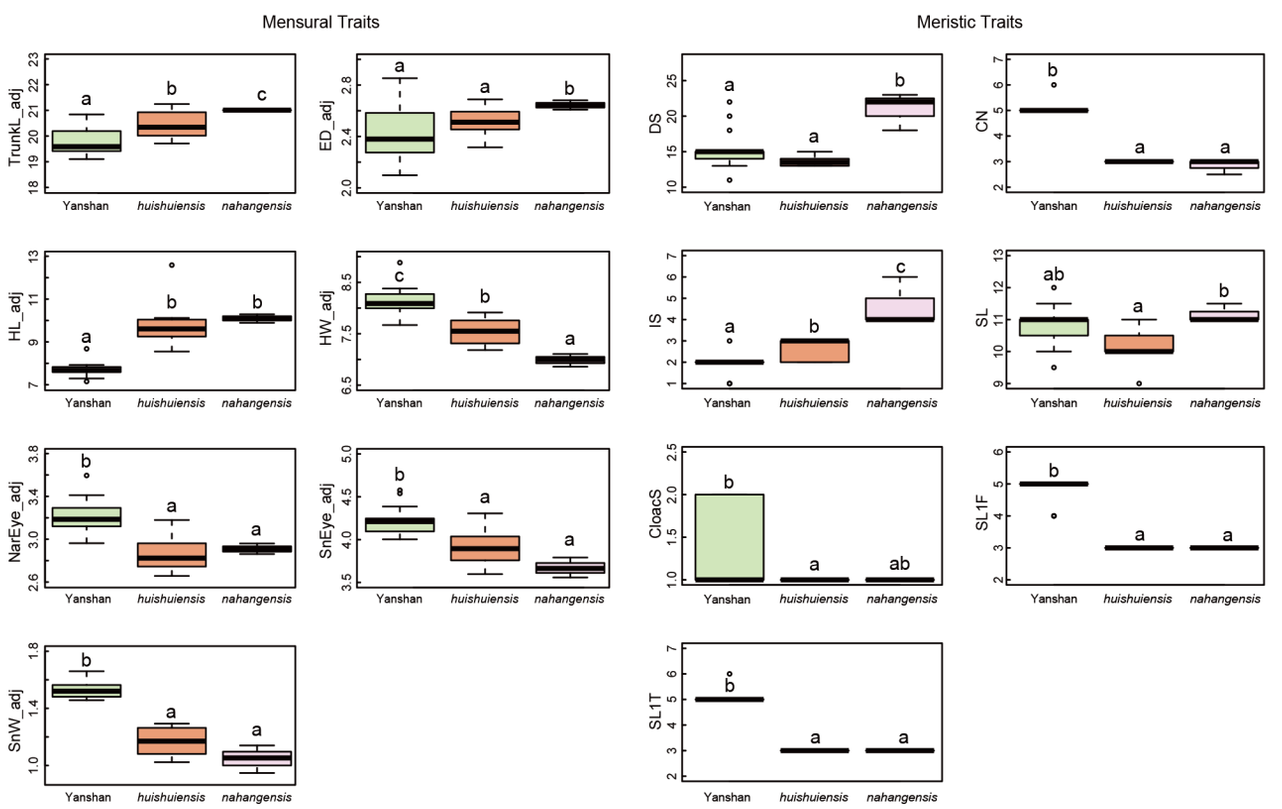

Figure 4 Differences in adjusted mensural (left) and meristic (right) traits between specimens from Yanshan population and closely related species (*H. huishuiensis* and *H. nahangensis*)

Significantly distinguished groups (P<0.05) are indicated by different letters.

Table 8 PERMANOVA pairwise comparisons of multi-trait space of compared species within clade 6

Pairs	F. Model	R2	*P*-value	*P*-adjusted	Sig
Yanshan – *huishuiensis*	23.1	0.549	<0.001	<0.001	***
Yanshan – *nahangensis*	20.6	0.595	0.002	0.003	**
huishuiensis – *nahangensis*	14.1	0.610	0.006	0.006	**

Sig: Significance levels. **: $P<0.01$; ***: $P<0.001$ (50 000 permutations).

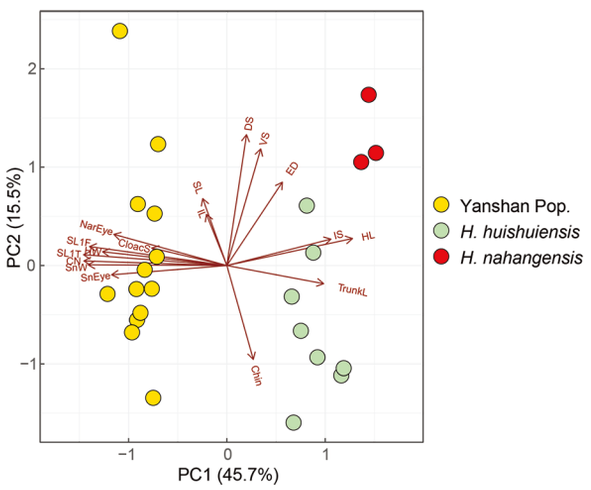

Figure 5 PCA of Yanshan population, *H. huishuiensis*, and *H. nahangensis* showing morphospatial relationships along first two components

Dots indicate positions of individuals in PCA morphospace and arrows indicate vectors for each morphological trait (acronyms for traits are indicated).

internasal scales 1–4; supralabial scales 8–12; infralabial scales 8–11; subdigital lamellae on fingers II–V (3 or 4)-(3–5)-(3–5)-(3 or 4); subdigital lamellae on toes II–V (3 or 4)-(3–5)-(3–5)-(3 or 4); dorsal scales 11–15; ventral scales 5–7; pale-gray base color on body, two lines of dark blotches running from neck to sacrum on dorsal side; dark postorbital stripe extending at least to base of neck; dorsolateral stripe indistinct or completely absent; ventrolateral stripe on trunk absent; dark postsacral markings bearing anteriorly projecting arms.

Description of holotype: Adult male, SVL 34.06 mm; head triangular in dorsal profile, depressed, distinct from neck (HL 6.03 mm; HW 6.77 mm); lores flat; snout long (SnEye 3.48 mm; SnEye/HL 58%) and narrow (SnW 1.26 mm; SnW/HW 19%); eyes large (ED 1.96 mm; ED/HL 33%); rostral scale wider than high, bordered posteriorly by two large supranasals and three internasals (IS); nares bordered anteriorly by rostral scale, ventrally by first supralabial scale, dorsally by supranasal scale, posteriorly by three postnasals; supralabials square, 10/9 (left/right), tapering from rostral to point in line with posterior margin of orbit (SL); infralabials square, 10/9 (left/right), tapering from mental to point in line with posterior margin of orbit (IL); scales on head small, rounded, largest on rostrum; mental triangular, bordered by first infralabials and posteriorly by two enlarged postmentals; each postmental bordered anterolaterally by first infralabial; eight chin scales touching internal edges of infralabials from juncture of 2nd and 3rd infralabial scales on left of mental scale to same juncture on right (Chin); scales in gular region rounded, non-overlapping, becoming larger and more ovoid on venter. Body type robust and small, (TrunkL/SVL 49%), dorsoventrally compressed; dorsal body scales small, granular, 12 dorsal scales at midbody contained within one eye diameter; ventral body scales smooth and flat, much larger than dorsal scales, subimbricate, seven ventral scales at midbody contained within one eye diameter; forelimbs relatively short, covered dorsally with granular, subimbricate scales, smaller smooth scales ventrally; palmar scales flat, unevenly shaped, non-overlapping; finger I vestigial, clawless, fingers II–V well developed; proximal subdigital lamellae undivided, rectangular; distal subdigital lamellae divided and undivided, angular, U-shaped, except terminal lamellae rounded, undivided; lamellar formula on fingers II–V (3)-(4)-(4)-(3) on both hands; claws on fingers II–V well developed, unsheathed, strongly curved; hind limbs short, covered dorsally with granular, subimbricate scales, smaller smooth scales ventrally; plantar scales flat, unevenly shaped, non-overlapping; toe I vestigial, clawless, toes II–V well developed; proximal subdigital lamellae undivided, rectangular; distal subdigital lamellae divided and undivided, angular, U-shaped, except terminal lamellae rounded, undivided; lamellar formula on toes II–V (3)-(4)-(4)-(4) on both feet; claws on toes II–V well developed, unsheathed, strongly curved; one cloacal spur (CloacS) on each side; tail long, original (TL 32.32 mm; TL/SVL 94%), round in cross-section, dorsal scales on tail

Table 9 Test results for group separation of compared species within clade 6 along first two PCA axes (PC1 and PC2)

PC	Group pairwise	Estimate	*SE*	*df*	t. ratio	*P*-value	Sig
1	Yanshan – *huishuiensis*	–4.90	0.208	21	–23.581	<0.001	***
	Yanshan – *nahangensis*	–6.46	0.296	21	–21.811	<0.001	***
	huishuiensis – *nahangensis*	–1.56	0.313	21	–4.984	<0.001	***
2	Yanshan – *huishuiensis*	1.13	0.612	21	1.840	0.1812	NS
	Yanshan – *nahangensis*	–2.01	0.872	21	–2.300	0.0778	NS
	huishuiensis – *nahangensis*	–3.13	0.922	21	–3.398	0.0073	**

PCA scores for each axis were grouped by species and compared pairwise using Tukey HSD tests to adjust for multiple comparisons. Sig: Significance levels. NS: Not significant. **: $P<0.01$; ***: $P<0.001$.

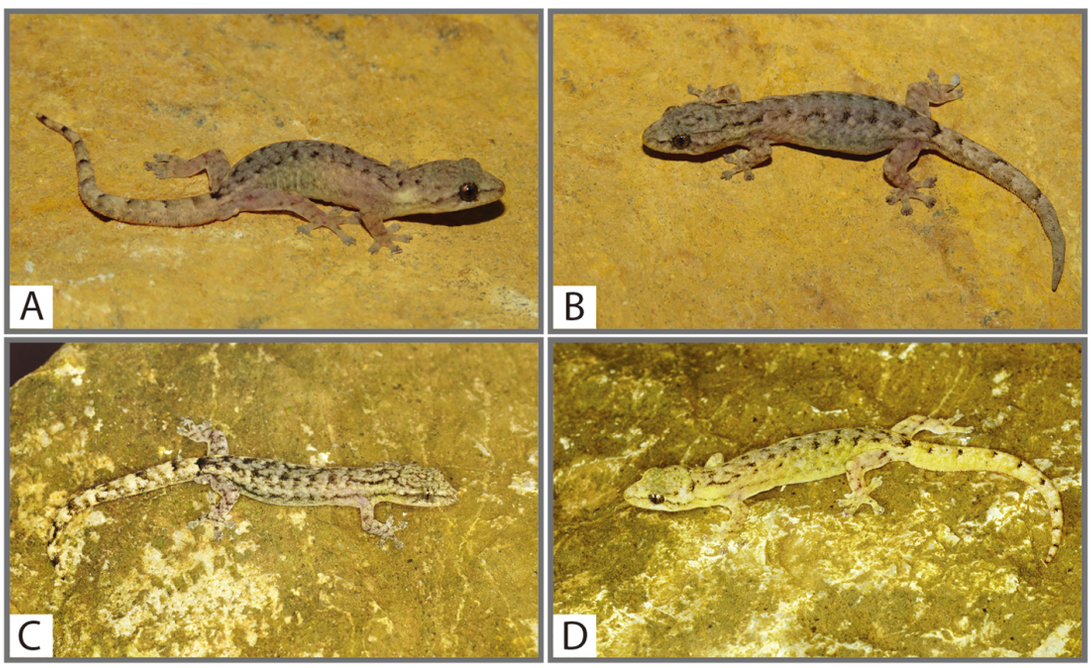

Figure 6 ***Hemiphyllodactylus simaoensis*** **sp. nov.**

A: Holotype, KIZ 062064, male in life; B: Paratype, KIZ 062065, female, in life; C: Paratype, KIZ 062072, male in life; D: Paratype, KIZ 062076, female in life. A and B were collected in Simao District (photos by Ade P. Agung), C and D were collected in Ning'er County (photos by Evan S. H. Quah).

larger than on body and head, smaller than subcaudals, no plate-like subcaudal scales.

Coloration in life (Figure 6): All *Hemiphyllodactylus* species can change the intensity and boldness of their coloration and patterns. The description below was taken when the holotype was photographed in the morning after capture. Base color of dorsal side of head, body, and limbs pale-gray, with two lines of dark blotches running from neck to sacrum on back; no dark marking on top of head; thin and indistinct dark pre- and postorbital stripes extending from external nares, through eye to just anterior of forelimb insertion on body; dark postsacral marking bearing anteriorly projecting arms; limbs with irregularly shaped, diffuse, and indistinct dark markings; dorsal side of tail with brown to black banded pattern; abdomen unicolor gray.

Variation: Coloration of this species varies considerably (Figure 6). Variations in mensural and meristic data are presented in Supplementary Table S7.

Distribution: *Hemiphyllodactylus simaoensis* **sp. nov.** is currently only known from Simao District and Ning'er County, Pu'er City, Yunnan Province, China.

Natural history: The holotype and seven paratypes (KIZ 062063, KIZ 062065–KIZ 062070) were collected on the evening of 6 July 2019 from a wall of a vacant building rarely used by humans in a forested karst area. The left and right sides of the building were densely covered by shrubs and trees. The back of the building was bordered by forested karst hills. The front of the building faced an old basketball court with several artificial lights, with the main road located further in front (Figure 7). The other 14 paratypes from Ning'er

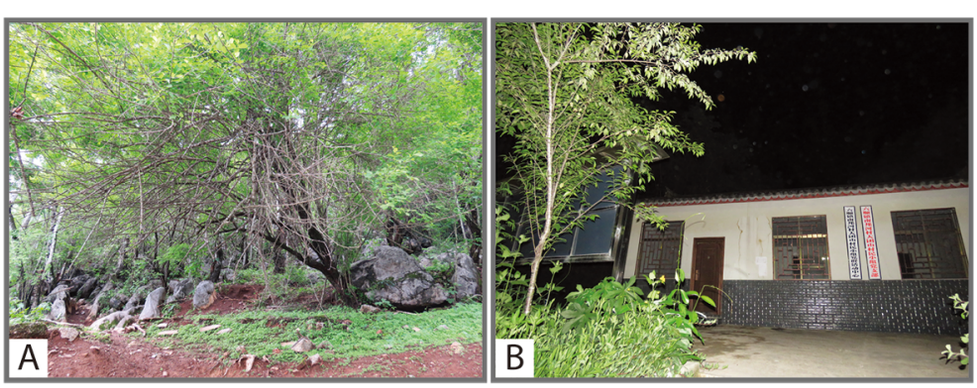

Figure 7 Habitat of ***Hemiphyllodactylus simaoensis*** **sp. nov.**

View of karst area in Simao District (A) and building where specimens KIZ 062063–KIZ 062070 were collected (B) (photos by Ade P. Agung).

County (KIZ 062072–KIZ 062077, KIZ 062079–KIZ 062084, KIZ 062087–KIZ 062088) were collected one year earlier, on the evenings of 16 and 17 August 2018, from a cement wall in a forested karst area.

Etymology: The specific epithet *simaoensis* refers to the name of the district where the holotype originates, Simao District, Pu'er City, Yunnan Province, China.

Morphological comparisons: A full list of trait comparisons is provided in Supplementary Table S3. Here, we describe morphological variations in *Hemiphyllodactylus simaoensis* **sp. nov.** and differences from its congeners for traits that differed between species. However, in terms of the range of trait values, *Hemiphyllodactylus simaoensis* **sp. nov.** was indistinguishable from the *H. jinpingensis* specimen examined but distinct from *H. jinpingensis* reported in Guo et al. (2015) (Supplementary Table S3). We consider this to be an artifact of researcher bias in the way data were taken. In terms of body ratios, *Hemiphyllodactylus simaoensis* **sp. nov.** differs from *H. jinpingensis* (values obtained from Guo et al. (2015)), *H. montawaensis*, *H. tonywhitteni*, and *H. ngwelwini* by shorter head (HL/SVL), wider head (HW/HL), greater SnEye distance (SnEye/HL), greater NarEye distance (NarEye/HL), larger eyes (ED/HL), and wider snout (SnW/HL) (Table 10).

In terms of scalation, the new species differs from *H. montawaensis*, *H. tonywhitteni*, and *H. ngwelwini* by fewer VS (5–7 vs. 7 or 8, 7–9, 7 or 8, respectively), and differs from *H.*

Table 10 Key trait differences between *Hemiphyllodactylus simaoensis* sp. nov. and its congeners

	H. jinpingensis	*H. montawaensis*	*H. tonywhitteni*	*H. ngwelwini*	*H. simaoensis* **sp. nov.**
HL/SVL	0.23–0.24	0.23–0.26	0.24–0.27	0.19–0.26	0.16–0.20
HW/HL	0.73–0.76	0.68–0.73	0.62–0.74	0.81–0.94	0.98–1.18
SnEye/HL	0.41–0.43	0.41–0.44	0.41–0.50	0.41–0.54	0.52–0.63
NarEye/HL	0.29–0.32	0.29–0.34	0.29–0.34	0.28–0.41	0.38–0.46
ED/HL	0.22–0.26	0.22–0.24	0.21–0.23	0.23–0.31	0.30–0.35
SnW/HL	0.13–0.15	0.13–0.15	0.13–0.14	0.14–0.18	0.18–0.24

Values for *H. jinpingensis* were obtained from Guo et al. (2015), *H. montawaensis* and *H. tonywhitteni* were from Grismer et al. (2017), and *H. ngwelwini* was from Grismer et al. (2020a). See text for abbreviations.

Figure 8 Variations in color and patterns of *Hemiphyllodactylus yanshanensis* sp. nov.

A: Holotype, KIZ 062090, male, in life; B: Paratype, KIZ 062091, female, in life; C: Paratype, KIZ 062092, female, in life; D: Paratype, KIZ 062093, female, in life (photos by Ade P. Agung).

tonywhitteni by more CN (5 or 6 vs. 3–5). For body coloration and pattern, the new species differs from *H. montawaensis* by presence of dark transverse blotches on dorsum (vs. reticulate pattern). The new species differs from *H. tonywhitteni* by presence of dark transverse blotches on dorsum (vs. absent) and absence of light-colored dorsolateral spots on trunk (vs. present). The new species differs from *H. ngwelwini* by presence of dark transverse blotches on dorsum (vs. absent) (see Supplementary Table S3 for all comparative values).

***Hemiphyllodactylus yanshanensis* sp. nov. (Figure 8)**

Suggested English name: Yanshan slender gecko

Suggested Chinese name: 砚山半叶趾虎

Holotype: Adult male (KIZ 062090) collected on 1 July 2019 by Ade P. Agung, Jian-Mei Lu, and Zong-Bao Yang from forested karst hills in Yanshan County, Yunnan Province, China (N23.61680°, E104.41669°; 1 536 m a.s.l.).

Paratypes: Nine adult females (KIZ 062091–KIZ 062096, KIZ 062100–KIZ 062102) and three adult males (KIZ 062097–KIZ 062099), same data as holotype.

Diagnosis: *Hemiphyllodactylus yanshanensis* **sp. nov**. can be distinguished from all congeners by a unique combination of the following characters: maximum SVL 46.28 mm; chin scales 8–11; enlarged postmentals; circumnasal scales 5–6; internasal scales 1–3; supralabial scales 9–12; infralabial scales 9–12; ventral scales 7–13; dorsal scales 11–22; subdigital lamellae on fingers II–V (4 or 5)-(5–7)-(5–7)-(4 or 5); subdigital lamellae on toes II–V (4 or 5)-(5 or 6)-(5–7)-(5 or 6); subdigital lamellae wider than long on first finger (4 or 5); subdigital lamellae wider than long on first toe (5 or 6); pale brown color base on body with various transverse blotched patterns on dorsum; dark postorbital stripe extending at least to base of neck; dorsolateral stripe on trunk present; ventrolateral stripe on trunk absent; postsacral marking bearing anteriorly projecting arms.

Description of holotype: Adult male, SVL 40.03 mm; head triangular in dorsal profile, depressed, distinct from neck (HL 7.27 mm; HW 7.68 mm); lores flat; snout long (SnEye 4.07 mm; SnEye/HL 56%) and narrow (SnW 1.52 mm; SnW/HW 20%); eyes large (ED 2.27 mm; ED/HL 31%); rostral scale wider than high, bordered posteriorly by two large supranasals and two internasals (IS); nares bordered anteriorly by rostral scale, ventrally by first supralabial scale, dorsally by supranasal scale, posteriorly by three postnasals; supralabials square, 9/10 (left/right), tapering from rostral to point in line with posterior margin of orbit (SL); infralabials square, 10/10 (left/right), tapering from mental to point in line with posterior margin of orbit (IL); scales on head small, rounded, largest on rostrum; mental triangular, bordered by first infralabials and posteriorly by two enlarged postmentals; each postmental bordered anterolaterally by first infralabial; nine chin scales touching internal edges of infralabials from juncture of 2nd and 3rd infralabial scales on left of mental scale to same juncture on right (Chin); scales in gular region rounded, non-overlapping, becoming larger and more ovoid on venter. Body type robust and small (TrunkL/SVL 47%), dorsoventrally compressed; dorsal body scales small, granular, 14 dorsal scales at midbody contained within one eye diameter; ventral body scales smooth and flat, much larger than dorsal scales, subimbricate, eight ventral scales at midbody contained within one eye diameter; forelimbs relatively short, covered dorsally with granular, subimbricate scales, smaller smooth scales ventrally; palmar scales flat, unevenly shaped, non-overlapping; finger I vestigial, clawless, fingers II–V well developed; proximal subdigital lamellae undivided, rectangular; distal subdigital lamellae divided and undivided, angular, U-shaped, except terminal lamellae rounded, undivided; lamellar formula on fingers II–V (4)-(5)-(5)-(4) on both hands; claws on fingers II–V well developed, unsheathed, strongly curved; hind limbs short, covered dorsally with granular, subimbricate scales, smaller smooth scales ventrally; plantar scales flat, unevenly shaped, non-overlapping; toe I vestigial, clawless, toes II–V well developed; proximal subdigital lamellae undivided, rectangular; distal subdigital lamellae divided and undivided, angular, U-shaped, except terminal lamellae rounded, undivided; lamellar formula on toes II–V (4)-(5)-(5)-(5) on left foot and (4)-(6)-(6)-(5) on right foot; claws on toes II–V well developed, unsheathed, strongly curved; one cloacal spur (CloacS) on each side; tail long, original (TL 34.01 mm; TL/SVL 85%), round in cross-section, dorsal scales on tail larger than on body and head, smaller than subcaudals, no plate-like subcaudal scales.

Coloration in life (Figure 8): All *Hemiphyllodactylus* species can change the intensity and boldness of their coloration and patterns. The description below was taken when the holotype was photographed in the morning after capture. Base color of dorsal side of head, body, and limbs pale-brown and densely mottled with darker markings; top of head overlain with indistinct blotches; indistinct pre- and postorbital stripes extending from external nares, through eye to just anterior of forelimb insertion on body; postsacral marking bearing anteriorly projecting arms; limbs with irregularly shaped, diffuse, dark markings; tail pale-gray, with several irregularly shaped dark markings on dorsal side, diffused on lateral sides; abdomen unicolor gray.

Variation: Coloration of this species varies considerably (Figure 8). Variations in mensural and meristic data are presented in Supplementary Table S8.

Distribution: *Hemiphyllodactylus yanshanensis* **sp. nov.** is only known from the type locality in Yanshan County, Yunnan Province, China (Figure 9).

Natural history: All specimens were collected during the evening of 1 July 2019 on the surface of a forested karst hill in Yanshan County, Yunnan Province, China (Figure 10). There were several gravid females among the specimens collected, each containing two eggs. We also found two eggs placed together loosely in the crevices of the same hill, which we assumed were laid by *Hemiphyllodactylus yanshanensis* **sp. nov.** based on their size (Figure 10), indicating that its reproductive season extends into July (see reports on other *Hemiphyllodactylus* species in Cobos et al. (2016) and Grismer et al. (2015)). The karst hills were surrounded by paddy fields and several huts and houses were nearby.

Etymology: The specific epithet *yanshanensis* refers to the name of Yanshan County where the specimens were found.

Morphological comparisons: A full list of trait comparisons is provided in Supplementary Table S5. Here, we describe morphological variations in *Hemiphyllodactylus yanshanensis* **sp. nov.** and differences from *H. huishuiensis* and *H.*

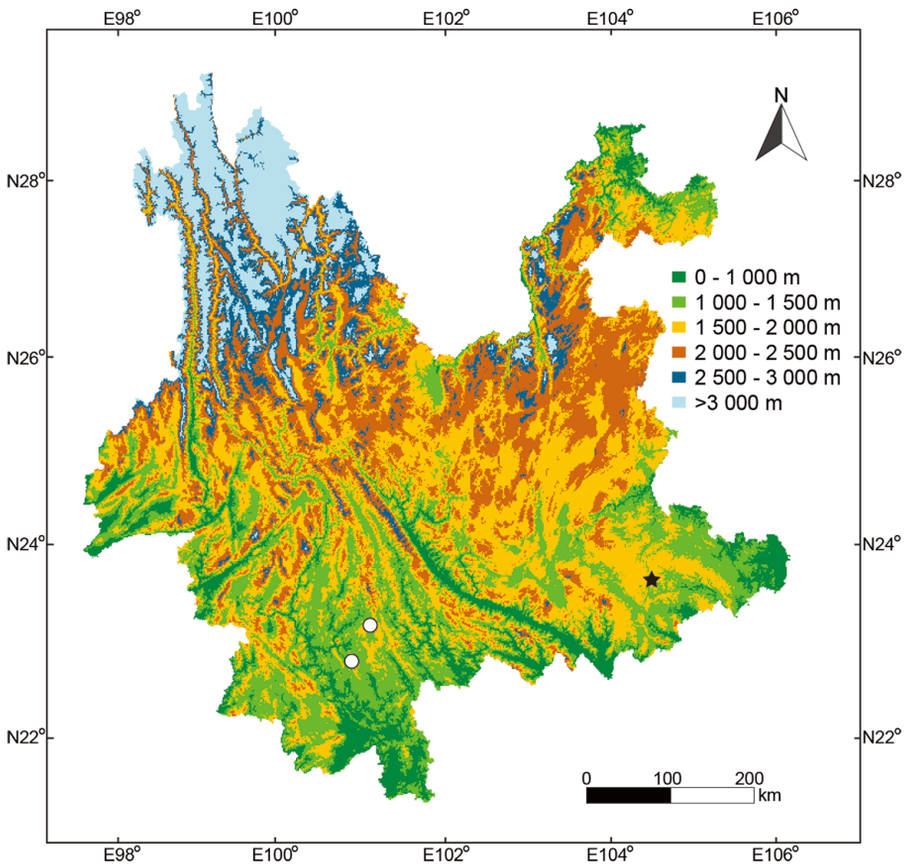

Figure 9 Map of Yunnan with type localities of *Hemiphyllodactylus simaoensis* sp. nov. (white circles) and *Hemiphyllodactylus yanshanensis* sp. nov. (black star)

Color in map indicates altitude, other species are not shown due to potential for further undescribed cryptic species.

nahangensis for traits that differed between species. In terms of body ratios, *Hemiphyllodactylus yanshanensis* **sp. nov.** differs from *H. huishuiensis* and *H. nahangensis* by shorter head (HL/SVL), wider head (HW/HL), greater SnEye distance (SnEye/HL), greater NarEye distance (NarEye/HL), larger eyes (ED/HL), and wider snout (SnW/HL) (Table 11).

In terms of scalation, the new species differs from *H. huishuiensis* and *H. nahangensis* by more circumnasal scales (5 or 6 vs. 3 and 2 or 3, respectively) and more subdigital lamellae wider than long on first finger and toe (SL1F=4 or 5 vs. 3; SL1T=5 or 6 vs. 3). Furthermore, the new species also differs from *H. nahangensis* by fewer internasal scales (IS=1–3 vs. 4–6) and fewer femoroprecloacal pores or pitted scales in females (10–16 vs. 22–24). In coloration, the new species differs from *H. huishuiensis* by presence of light-colored dorsolateral spots on trunk (vs. absent). It also differs from *H. nahangensis* by presence of dark postorbital stripe and dark transverse dorsal blotches (vs. absent) (see Supplementary Table S5 for all comparative values).

DISCUSSION

Diversity of *Hemiphyllodactylus* in southern Chinese karsts

Most Chinese specimens of *Hemiphyllodactylus* were previously identified as *H. yunnanensis* Boulenger 1903. In 2013, however, Grismer et al. (2013) conducted an integrative taxonomic study and revealed that this taxon is much more diverse than previously reported. A number of species have since been described in China. Most recently, *H. zhutangxiangensis* was described from Lancang Lahu Autonomous County (Agung et al., 2021) and *H. zayuensis* was described from Zayu County, Tibet (Che et al., 2020), with both species considered likely members of clade 3, given that all members are distributed in western Yunnan and northern Myanmar. The population in Dao County, Hunan Province, was also recently identified as *H. dupanglingensis* (Zhang et al., 2020) and as sister to *H. zugi*, a species that occurs on the border of Vietnam and Guangxi Province, China (Nguyen et al., 2013). Both are members of clade 6, together with *H. hongkongensis* (Sung et al., 2018), *H. dushanensis* (Zhou et al., 1981), and *H. huishuiensis* (Yan et al., 2016), which occur in southeastern China. Thus, together with *H. yunnanensis*, *H. longlingensis*, *H. jinpingensis*, *H. changningensis* (Guo et al., 2015), and *H. typus* Bleeker (Uetz et al., 2021), a total of 12 species are currently known in China. However, given the extensive and unsurveyed karst habitat across southern China, many more species are likely to be discovered.

Mitochondrial *ND2* analysis indicated that

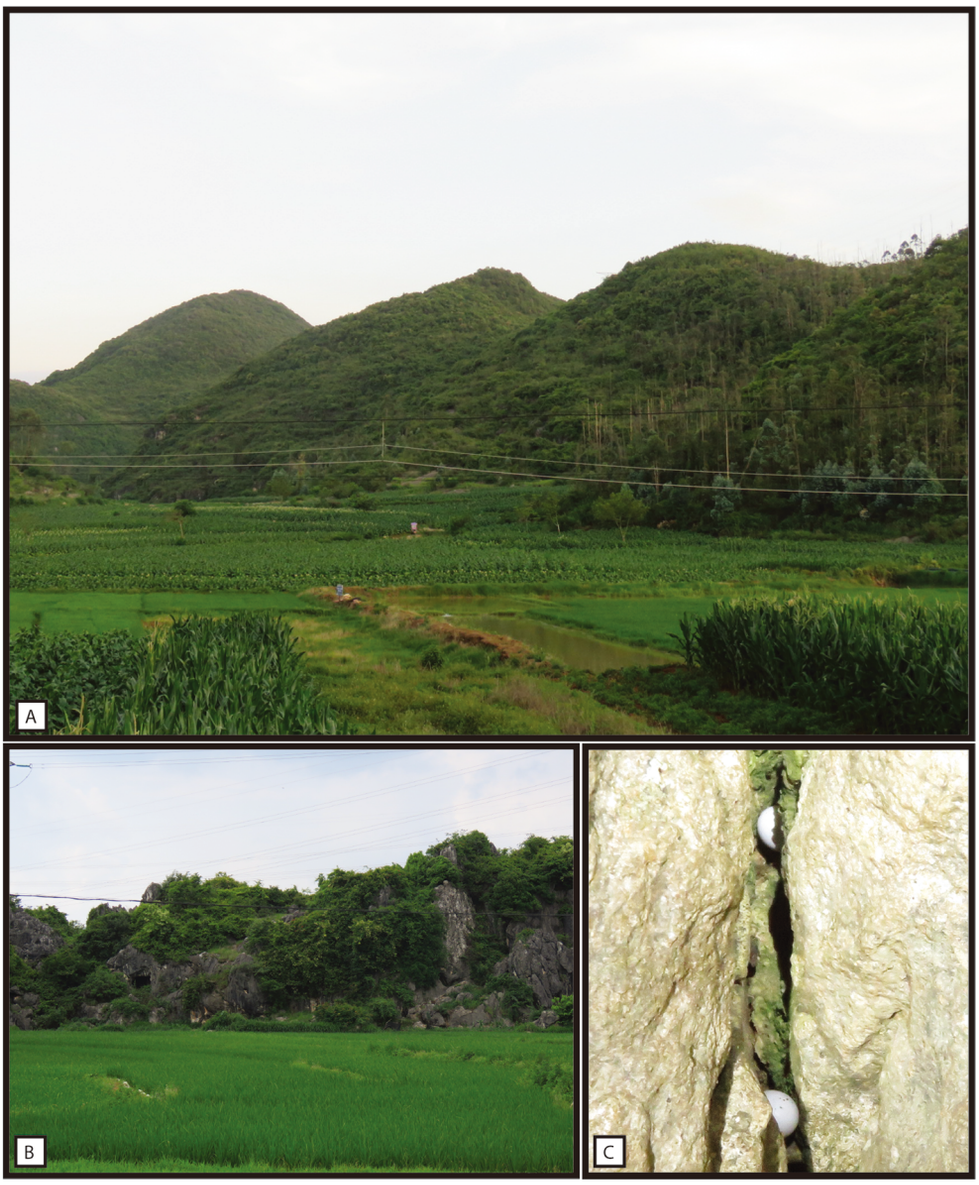

Figure 10 Habitat of *Hemiphyllodactylus yanshanensis* sp. nov.

A: View of karst hills in Yanshan County, Yunnan, China; B: Karst hill where specimens were spotted; C: Deposited eggs of *Hemiphyllodactylus yanshanensis* **sp. nov.** in karst crevices (photos by Ade P. Agung).

Table 11 Key trait differences between *Hemiphyllodactylus yanshanensis* sp. nov. and its congeners

	H. huishuiensis	*H. nahangensis*	*H. yanshanensis* **sp. nov.**
HL/SVL	0.21–0.29	0.24	0.17–0.21
HW/HL	0.61–0.84	0.69	1.02–1.16
SnEye/HL	0.31–0.45	0.36–0.39	0.51–0.60
NarEye/HL	0.22–0.34	0.28–0.31	0.39–0.44
ED/HL	0.20–0.28	0.24–0.27	0.29–0.36
SnW/HL	0.10–0.14	0.10–0.12	0.18–0.22

See text for abbreviations.

Hemiphyllodactylus simaoensis **sp. nov.** and *Hemiphyllodactylus yanshanensis* **sp. nov.** are members of clades 4 and 6, respectively, and are embedded within the *typus* group. *Hemiphyllodactylus simaoensis* **sp. nov.** appears to be most closely related to *H. jinpingensis* (6.3%; Table 2) in clade 4, with most members of this clade distributed on Shan Plateau, eastern Myanmar. *Hemiphyllodactylus yanshanensis* **sp. nov.** appears to be most closely related to *H. huishuiensis*

from southeastern China (4.3%; Table 3) in clade 6. These distributions and relationships highlight the complex biogeography of Yunnan. The discovery of these two new species increases the total number of *Hemiphyllodactylus* species in China to 14, four of which have been described in the last five years. Thus, further research is required as many species likely remain to be discovered in China and other parts of Asia.

Our Yunnan samples were nested in four different clades (clades 3, 4, 6 and 7; Figure 1), suggesting that Yunnan may have been colonized on at least four separate occasions, as the sister species to clades 3 and 4 (*H. khlonglanensis*) and clades 6 and 7 (*H. pardalis*) are only known from Thailand. Nevertheless, more population data are needed to determine if the splits between clades 3 and 4 and clades 6 and 7 occurred before or after colonization of Yunnan.

The description of *Hemiphyllodactylus yanshanensis* **sp. nov.** in this paper is the first evidence of colonization in Yunnan by a member of clade 6, with most clade members occurring in eastern Indochina (Vietnam and eastern Laos) and southeastern China (Guizhou, Hunan, and Hongkong SAR). These species discoveries emphasize that *Hemiphyllodactylus* diversity within China and neighboring regions is underestimated.

Trait reliability

The newly described species (*Hemiphyllodactylus simaoensis* **sp. nov.** and *Hemiphyllodactylus yanshanensis* **sp. nov.**) differed significantly in several morphological traits from their sister species (see Results). Nevertheless, these morphological traits are challenging to use in the field without specimen comparisons, and thus, obtaining tissue samples for genetic analysis is crucial to corroborate what is noted in the field. The use of integrated taxonomic approaches with genetic and morphological data, coupled with robust statistical analyses, will increase the accuracy of species delimitation. Therefore, given that many species in *Hemiphyllodactylus* are morphologically convergent and cryptic (Grismer et al., 2013), single morphological evidence may not be sufficient for species identification in *Hemiphyllodactylus.*

Conservation implications

Our study suggests that karst regions in Yunnan, which cover nearly 44% of the province (Nester, 2021), are likely to harbor additional undescribed species of *Hemiphyllodactylus*. However, despite the recent delineation of geoparks (e.g., Shilin, Dali-Cangshan), these hotspots of endemism are disproportionately under-protected. Furthermore, *H. yunnanensis* may be a species complex (clade 7) and require further taxonomic revision. Based on this preliminary analysis, we hypothesize that *Hemiphyllodactylus* in the karst regions of Yunnan has had a complex colonization history, given that we potentially found multiple species in one site as well as one species distributed in multiple karst hills (Agung et al., unpublished data).

The continuation of species discoveries with increasing field surveys may clarify the status of isolated populations of *Hemiphyllodactylus* species groups. Karst outcrops provide biodiversity arks and focal points for speciation (Clements et al., 2006; Grismer et al., 2021), with a high degree of isolation for *Hemiphyllodactylus* populations. Due to their poor dispersal abilities, different populations in different karst areas may have evolved into separate lineages, and thus could be recognized as distinct species (Grismer, 1999). Considering the allopatric populations of *Hemiphyllodactylus*, with presumably no or low rates of gene flow among them, they may have become phenetically and genetically distinguishable over time (as reviewed in de Queiroz, 2007). In the last 10 years, approximately 31 new species have been identified throughout Asia, with each species usually described from a single karst area or complex (i.e., Grismer et al., 2020a), highlighting the high rate of local *Hemiphyllodactylus* endemism in each karst region. *Hemiphyllodactylus simaoensis* **sp. nov.** and *Hemiphyllodactylus yanshanensis* **sp. nov.** exhibited clear genetic and phenotypic differences from their sister lineages, *H. jinpingensis* (located more than 200 km away) and *H. huishuiensis* (located more than 350 km away), respectively, thus supporting the assumption of high local endemism for each karst region, even though some areas may have multiple sympatric species. High endemism in karst geckos is not only reported for *Hemiphyllodactylus*, but also for *Cyrtodactylus* (Davis et al., 2019; Grismer et al., 2021; Luu et al., 2016; Nazarov et al., 2018; Nguyen et al., 2017; Pauwels et al., 2016) and *Cnemaspis* (Grismer et al., 2014; Wood et al., 2017). In addition, high numbers of endemic flora and invertebrates have also been reported from limestone forest habitats (Clements et al., 2006; Marzuki et al., 2021; Nguyen et al., 2021). However, the genus *Hemiphyllodactylus* remains understudied and increased survey efforts with broader geographic coverage will likely increase the number of new species discovered. Notably, many karsts still lack inventories and given the high rate of endemism, much work is needed to map taxa across the region and develop appropriate plans for protection and representative coverage of species across this naturally fragmented system.

Neglected habitats, such as karst ecosystems, require in-depth investigation and survey. Quantifying the biodiversity of a region also requires accurate taxonomy, as species are the fundamental units of conservation planning (Mace, 2004). Conserving karst landscapes and the communities that depend upon them cannot be achieved without adequate knowledge of existing species. Major threats to gecko species, including the two described here, are habitat destruction from quarrying and deforestation. Furthermore, with the rapid rate of karst loss across much of Southeast Asia, failure to identify and map the ranges of species may ultimately mean species become extinct without formal description. Therefore, appropriate conservation management plans are needed to reduce the loss of key habitats and risk of potential invasion by non-native species. Without identifying species, understanding their ranges, and increasing systematic surveys of these diverse and complex regions, the extinction of species may occur before they are described, or we may only observe specimens whose habitats have already been destroyed. Mapping the distributions of range-limited herptiles and understanding their vulnerabilities are crucial factors for targeted management and conservation. For example, research on the Chinese salamander (*Andrias jiangxiensis*,

Chai et al., 2022) has highlighted how few sites retain the species, underscoring the need for the identification and protection of these sites. Our study and that of Chai et al. (2022) demonstrate the need for an integrated approach, including genetics and morphology, to identify species and form the basis for management and conservation. Therefore, further work is urgently needed to understand cryptic distributions and enable targeted management.

Synthesis and future directions

Prior to 2021, only 12 species of *Hemiphyllodactylus* were known in southern China. Recent studies have transformed our knowledge regarding the group and added new species based on a variety of different traits and molecular data. However, these recent studies also highlight the need to better understand regional diversity patterns and biogeography and provide a basis for future management and conservation given the high rates of habitat loss across the range. The description of multiple species from Yunnan in the last 10 years also emphasizes the need to redouble our efforts to ensure sufficient representation in sampling. Furthermore, given the lack of any single trait to differentiate between species (and the need to analyze multiple traits simultaneously), integration of morphological and genetic analyses is required to better identify species, although field identification may continue to be a challenge. Key regions where we expect high complexity in species populations (due to high environmental heterogeneity forming barriers to gene flow) include the Yuanjiang valley and Ailao mountain range in Yunnan. Studies in countries such as Malaysia and Myanmar have demonstrated high levels of regional endemism within the group, indicating that more work is needed to sample and describe *Hemiphyllodactylus* in Yunnan. Without knowledge of where species are found, developing effective and efficient management will remain difficult. Given the rate of species description in this neglected taxon, as well as the high rates of habitat loss, further research is needed to describe species and map their ranges before they can be protected, especially for genera with high levels of site-specific endemism in inventory-poor areas.

NOMENCLATURAL ACTS REGISTRATION

The electronic version of this article in portable document format will represent a published work according to the International Commission on Zoological Nomenclature (ICZN), and hence the new names contained in the electronic version are effectively published under that Code from the electronic edition alone (see Articles 8.5–8.6 of the Code). This published work and the nomenclatural acts it contains have been registered in ZooBank, the online registration system for the ICZN. The ZooBank LSIDs (Life Science Identifiers) can be resolved and the associated information can be viewed through any standard web browser by appending the LSID to the prefix http://zoobank.org/.

Publication LSID: urn:lsid:zoobank.org:pub:763DE16C-BA54-41ED-910A-F0423AA62A98.

Nomenclatural act LSID for *Hemiphyllodactylus simaoensis* **sp. nov.**: urn:lsid:zoobank.org:act:A863C059-F959-4450-BCD9-6DF3B92D5E68.

Nomenclatural act LSID for *Hemiphyllodactylus yanshanensis* **sp. nov.**: urn:lsid:zoobank.org:act:02D7C54D-EFEC-4225-8649-BC1D7FED3617.

SCIENTIFIC FIELD SURVEY PERMISSION INFORMATION

The Ethics Committee of Xishuangbanna Tropical Botanical Garden, Chinese Academy of Sciences, approved the study and provided ethics permission. All local regulations were followed in the collection of samples and specimens for the study.

SUPPLEMENTARY DATA

Supplementary data to this article can be found online.

COMPETING INTERESTS

The authors declare that they have no competing interests

AUTHORS' CONTRIBUTIONS

A.P.A., L.L.G., J.L.G., A.C.H. designed the study. A.P.A., A.C., L.L.G., J.L.G., E.S.H.Q., and J.M.L. collected data. A.P.A., A.C., and L.L.G. conducted phylogenetic analyses. A.P.A. examined morphology. A.P.A and K.W.T conducted statistical analyses. A.P.A. and E.S.H.Q. wrote the manuscript. A.P.A., L.L.G., and A.C.H. revised the manuscript. All authors read and approved the final version of the manuscript.

ACKNOWLEDGEMENTS

We thank Brian Folt, Myint Kyaw Thura, Zhong-Bao Yang, and Shi-Fu Pu for help during fieldwork, Tuanjit Sritongchuay for loaning equipment for specimen measurements, and Yan-Hua Chen and Zi-Nan Ding for help with administrative work.

REFERENCES

Agarwal I, Khandekar A, Giri VB, Ramakrishnan U, Karanth KP. 2019. The hills are alive with geckos! A radiation of a dozen species on sky islands across peninsular India (Squamata: Gekkonidae, *Hemiphyllodactylus*) with the description of three new species. *Organisms Diversity & Evolution*, **19**(2): 341−361.

Agung AP, Grismer LL, Grismer JL, Quah ESH, Chornelia A, Lu JM, et al. 2021. A new species of *Hemiphyllodactylus* Bleeker (Squamata: Gekkonidae) from Yunnan, China and its phylogenetic relationship to other congeners. *Zootaxa*, **4980**(1): 1−27.

Chai J, Lu CQ, Yi MR, Dai NH, Weng XD, Di MX, et al. 2022. Discovery of a wild, genetically pure Chinese giant salamander creates new conservation opportunities. *Zoological Research*, **43**(3): 469−480.

Che J, Jiang K, Yan F, Zhang YP. 2020. Amphibians and Reptiles in Tibet: Diversity and Evolution. Beijing: Science Press, 803.

Clements GR, Sodhi NS, Schilthuizen M, Ng PKL. 2006. Limestone karsts of Southeast Asia: imperiled arks of biodiversity. *BioScience*, **56**(9): 733−742.

Cobos A, Grismer LL, Wood Jr PL, Quah ESH, Anuar S, Muin MA. 2016. Phylogenetic relationships of geckos of the *Hemiphyllodactylus harterti* group, a new species from Penang Island, Peninsular Malaysia, and a likely case of true cryptic speciation. *Zootaxa*, **4107**(3): 367−380.

Conroy CJ, Papenfuss T, Parker J, Hahn NE. 2009. Use of Tricaine

Methanesulfonate (MS222) for Euthanasia of Reptiles. *Journal of the American Association for Laboratory Animal Science*, **48**(1): 28−32.

Davis HR, Bauer AM, Jackman TR, Nashriq I, Das I. 2019. Uncovering karst endemism within Borneo: two new *Cyrtodactylus* species from Sarawak, Malaysia. *Zootaxa*, **4614**(2): 331−352.

De Queiroz K. 2007. Species concepts and species delimitation. *Systematic Biology*, **56**(6): 879−886.

Dittmar K, Porter M, Price L, Svenson GJ, Whiting MF. 2005. A brief survey of invertebrates in caves of Peninsular Malaysia. *Malayan Nature Journal*, **57**(2): 221−233.

Do QH, Pham CT, Phan TQ, Le MD, Ziegler T, Nguyen TQ. 2020. A new species of *Hemiphyllodactylus* (Squamata: Gekkonidae) from Tuyen Quang Province, Vietnam. *Zootaxa*, **4821**(3): 511−532.

Eliades SJ, Phimmachak S, Sivongxay N, Siler CD, Stuart BL. 2019. Two new species of *Hemiphyllodactylus* (Reptilia: Gekkonidae) from Laos. *Zootaxa*, **4577**(1): 131−147.

Grismer LL. 1999. An evolutionary classification of reptiles on islands in The Gulf of California, Mexico. *Herpetologica*, **55**(4): 446−469.

Grismer LL, Wood Jr PL, Anuar S, Muin MA, Quah ESH, Mcguire JA, et al. 2013. Integrative taxonomy uncovers high levels of cryptic species diversity in *Hemiphyllodactylus* Bleeker, 1860 (Squamata: Gekkonidae) and the description of a new species from Peninsular Malaysia. *Zoological Journal of the Linnean Society*, **169**(4): 849−880.

Grismer LL, Wood Jr PL, Anuar S, Quah ESH, Muin MA, Onn CK, et al. 2015. Repeated evolution of sympatric, palaeoendemic species in closely related, co-distributed lineages of *Hemiphyllodactylus* Bleeker, 1860 (Squamata: Gekkonidae) across a sky-island archipelago in Peninsular Malaysia. *Zoological Journal of the Linnean Society*, **174**(4): 859−876.

Grismer LL, Wood Jr PL, Anuar S, Riyanto A, Ahmad N, Muin MA, et al. 2014. Systematics and natural history of Southeast Asian Rock Geckos (genus *Cnemaspis* Strauch, 1887) with descriptions of eight new species from Malaysia, Thailand, and Indonesia. *Zootaxa*, **3880**(1): 1−147.

Grismer LL, Wood Jr PL, Poyarkov NA, Le MD, Karunarathna S, Chomdej S, et al. 2021. Karstic landscapes are foci of species diversity in the world's third-largest vertebrate genus *Cyrtodactylus* Gray, 1827 (Reptilia: Squamata; Gekkonidae). *Diversity*, **13**(5): 183.

Grismer LL, Wood Jr PL, Quah ESH, Thura MK, Oaks JR, Lin A. 2020a. Four new Burmese species of *Hemiphyllodactylus* Bleeker (Squamata: Gekkonidae) from distantly related parapatric clades from the Shan Plateau and Salween Basin. *Zootaxa*, **4758**(1): 45−82.

Grismer LL, Wood Jr PL, Thura MK, Zin T, Quah ESH, Murdoch ML, et al. 2018a. Twelve new species of *Cyrtodactylus* Gray (Squamata: Gekkonidae) from isolated limestone habitats in east-central and southern Myanmar demonstrate high localized diversity and unprecedented microendemism. *Zoological Journal of the Linnean Society*, **182**(4): 862−959.

Grismer LL, Wood Jr PL, Thura MK, Zin T, Quah ESH, Murdoch ML, et al. 2018b. Phylogenetic taxonomy of *Hemiphyllodactylus* Bleeker, 1860 (Squamata: Gekkonidae) with descriptions of three new *species* from Myanmar. *Journal of Natural History*, **52**(13–16): 881–915.

Grismer LL, Wood Jr PL, Zug GR, Thura MK, Grismer MS, Murdoch ML, et al. 2018c. Two more new species of *Hemiphyllodactylus* Bleeker (Squamata: Gekkonidae) from the Shan Hills of eastern Myanmar (Burma). *Zootaxa*, **4483**(2): 295−316.

Grismer LL, Yushchenko PV, Pawangkhanant P, Naiduangchan M, Nazarov RA, Orlova VF, et al. 2020b. A new species of *Hemiphyllodactylus* Bleeker (Squamata; Gekkonidae) from Peninsular Thailand that converges in morphology and color pattern on *Pseudogekko smaragdinus* (Taylor) from the Philippines. *Zootaxa*, **4816**(2): 171−190.

Guo WB, Zhou KY, Yan J, Li P. 2015. A new species of *Hemiphyllodactylus* Bleeker, 1860 (Squamata: Gekkonidae) from western Yunnan, China. *Zootaxa*, **3974**(3): 377−390.

Hoang DT, Chernomor O, von Haeseler A, Minh BQ, Vinh LS. 2018. UFBoot2: improving the ultrafast bootstrap approximation. *Molecular Biology and Evolution*, **35**(2): 518−522.

Huang TF, Zhang PL, Huang XL, Wu T, Gong XY, Zhang YX, et al. 2019. A new cave-dwelling blind loach, *Triplophysa erythraea* sp. nov. (Cypriniformes: Nemacheilidae), from Hunan Province, China. *Zoological Research*, **40**(4): 331−336.

Huelsenbeck JP, Ronquist F, Nielsen R, Bollback JP. 2001. Bayesian inference of phylogeny and its impact on evolutionary biology. *Science*, **294**(5550): 2310−2314.

Hughes AC. 2017. Understanding the drivers of Southeast Asian biodiversity loss. *Ecosphere*, **8**(1): e01624.

Kalyaanamoorthy S, Minh BQ, Wong TKF, von Haeseler A, Jermiin LS. 2017. ModelFinder: fast model selection for accurate phylogenetic estimates. *Nature Methods*, **14**(6): 587−589.

Kleiber C, Zeileis A. 2008. Applied Econometrics with R. New York: Springer.

Kumar S, Stecher G, Tamura K. 2016. MEGA7: Molecular evolutionary genetics analysis version 7.0 for bigger datasets. *Molecular Biology and Evolution*, **33**(7): 1870−1874.

Lenth RV. 2021[2021-07-03]. Emmeans: estimated marginal means, aka least-squares means. R package version 1.7. 5.https://CRAN.R-project.org/package=emmeans/.

Lleonart J, Salat J, Torres GJ. 2000. Removing allometric effects of body size in morphological analysis. *Journal of Theoretical Biology*, **205**(1): 85−93.

Luu VQ, Bonkowski M, Nguyen TQ, Le MD, Schneider N, Ngo HT, et al. 2016. Evolution in karst massifs: cryptic diversity among bent-toed geckos along the Truong Son Range with descriptions of three new species and one new country record from Laos. *Zootaxa*, **4107**(2): 101−140.

Mace GM. 2004. The role of taxonomy in species conservation. *Philosophical Transaction of the Royal Society B*, **359**(1444): 711−719.

Macey JR, Larson A, Ananjeva NB, Fang Z, Papenfuss TJ. 1997. Two novel gene orders and the role of light-strand replication in rearrangement of the vertebrate mitochondrial genome. *Molecular Biology and Evolution*, **14**(1): 91−104.

Marzuki MEB, Liew TS, Mohd-Azlan J. 2021. Land snails and slugs of Bau limestone hills, Sarawak (Malaysia, Borneo), with the descriptions of 13 new species. *ZooKeys*, **1035**(7): 1−113.

Miller MA, Pfeiffer W, Schwartz T. 2010. Creating the CIPRES Science Gateway for inference of large phylogenetic trees. *In*: Proceedings of the 2010 Gateway Computing Environments Workshop (GCE). New Orleans: IEEE, 1–8.

Minh BQ, Nguyen MAT, von Haeseler A. 2013. Ultrafast approximation for phylogenetic bootstrap. *Molecular Biology and Evolution*, **30**(5): 1188−1195.

Nazarov RA, Pauwels OSG, Konstantinov EL, Chulisov AS, Orlov NL, Poyarkov Jr NA. 2018. A new karst-dwelling bent-toed gecko (Squamata: Gekkonidae: *Cyrtodactylus*) from Xiangkhoang Province, northeastern Laos. *Zoological Research*, **39**(3): 202−219.

Nester H. 2021[2021-09-15]. China's karst region: infographics. Circle of Blue,https://www.circleofblue.org/2010/world/chinas-karst-region-

infographics/.
Nguyen CH, Van Nguyen L, Nguyen KS, Egorov AA, Averyanov LV. 2021. *Hemiboea chanii* (Gesneriaceae), a new species from limestone areas of northern Vietnam. *PhytoKeys*, **183**(1): 108−114.
Nguyen LT, Schmidt HA, von Haeseler A, Minh BQ. 2015. IQ-TREE: a fast and effective stochastic algorithm for estimating maximum-likelihood phylogenies. *Molecular Biology and Evolution*, **32**(1): 268−274.
Nguyen TQ, Do QH, Ngo HT, Van Pham A, Pham CT, Le MD, et al. 2020. Two new species of *Hemiphyllodactylus* (Squamata: Gekkonidae) from Hoa Binh Province, Vietnam. *Zootaxa*, **4801**(3): 513−536.
Nguyen TQ, Lehmann T, Le MD, Duong HT, Bonkowski M, Ziegler T. 2013. A new species of *Hemiphyllodactylus* (Reptilia: Gekkonidae) from northern Vietnam. *Zootaxa*, **3736**(1): 89−98.
Nguyen TQ, Van Pham A, Ziegler T, Ngo HT, Le MD. 2017. A new species of *Cyrtodactylus* (Squamata: Gekkonidae) and the first record of *C. otai* from Son La Province, Vietnam. *Zootaxa*, **4341**(1): 25−40.
Oksanen J, Simpson GL, Blanchet FG, Kindt R, Legendre P, Minchin PR, et al. 2020[2020-09-20]. Vegan: community ecology package. R package version 2.6–2.https://CRAN.R-project.org/package=vegan/.
Pauwels OSG, Sumontha M, Bauer AM. 2016. A new bent-toed gecko (Squamata: Gekkonidae: *Cyrtodactylus*) from Phetchaburi Province, Thailand. *Zootaxa*, **4088**(3): 409−419.
Pinheiro J, Bates D, DebRoy S, Sarkar D, EISPACK Authors, Siem Heisterkamp, et al. 2020[2020-09-20]. Nlme: linear and nonlinear mixed effects models. R package version 3.1–158.https://CRAN.R-project.org/package=nlme/.
Quah ESH, Grismer LL, Anuar MSS. 2021. Conservation of Peninsular Malaysia's Karst Herpetofauna: a review of herpetological discoveries, research trends, and challenges. *Raffles Bulletin of Zoology*, **69**: 235−252.
R Core Team. 2020. R: A language and environment for statistical computing. R foundation for statistical computing, Vienna, Austria.https://www.R-project.org/.
Rambaut A, Drummond AJ, Xie D, Baele G, Suchard MA. 2018. Posterior summarization in Bayesian phylogenetics using Tracer 1.7. *Systematic Biology*, **67**(5): 901−904.
Ronquist F, Teslenko M, van der Mark P, Ayres DL, Darling A, Höhna B, et al. 2012. MrBayes 3.2: efficient Bayesian phylogenetic inference and model choice across a large model space. *Systematic Biology*, **61**(3): 539−542.
Sung YH, Lee WH, Ng HN, Zhang YJ, Yang JH. 2018. A new species of *Hemiphyllodactylus* (Squamata: Gekkonidae) from Hong Kong. *Zootaxa*, **4392**(2): 361−373.
Thorpe RS. 1975. Quantitative handling of characters useful in snake systematics with particular reference to intraspecific variation in the Ringed Snake *Natrix natrix* (L.). *Biological Journal of the Linnean Society*, **7**(1): 27−43.
Thorpe RS. 1983. A review of the numerical methods for recognising and analysing racial differentiation. *In*: Felsenstein J. Numerical Taxonomy. Berlin: Springer, 404–423.
Tian MY, Huang S. 2015. Two new species of cavernicolous trechines from southern China karst (Coleoptera: Carabidae: Trechinae). *Journal of cave and Karst Studies*, **77**(3): 152−159.
Trifinopoulos J, Nguyen LT, von Haeseler A, Minh BQ. 2016. W-IQ-TREE: a fast online phylogenetic tool for maximum likelihood analysis. *Nucleic Acids Research*, **44**(W1): W232−W235.
Turan C. 1999. A note on the examination of morphometric differentiation among fish populations: the Truss System. *Turkish Journal of Zoology*, **23**(3): 259−263.
Uetz P, Freed P, Aguilar R, Hošek J. 2021[2021-11-10]. The reptile database. http://www.reptile-database.org.
Vieites DR, Wollenberg KC, Andreone F, Köhler J, Glaw F, Vences M. 2009. Vast underestimation of Madagascar's biodiversity evidenced by an integrative amphibian inventory. *Proceedings of the National Academy of Sciences of the United States of America*, **106**(20): 8267−8272.
Whitten T. 2009. Applying ecology for cave management in China and neighbouring countries. *Journal of Applied Ecology*, **46**(3): 520−523.
Wilcox TP, Zwickl DJ, Heath TA, Hillis DM. 2002. Phylogenetic relationships of the Dwarf Boas and a comparison of Bayesian and bootstrap measures of phylogenetic support. *Molecular Phylogenetics and Evolution*, **25**(2): 361−371.
Wood PL Jr, Grismer LL, Aowphol A, Aguilar CA, Cota M, Grismer MS, et al. 2017. Three new karst-dwelling *Cnemaspis* Strauch, 1887 (Squamata; Gekkoniade) from Peninsular Thailand and the phylogenetic placement of *C. punctatonuchalis* and *C. vandeventeri*. *PeerJ*, **5**: e2884.
Yan J, Lin YB, Guo WB, Li P, Zhou KY. 2016. A new species of *Hemiphyllodactylus* Bleeker, 1860 (Squamata: Gekkonidae) from Guizhou, China. *Zootaxa*, **4117**(4): 543−554.
Zhang B, Qian TY, Jiang XJ, Cai B, Deng XJ, Yang DD. 2020. A new species of *Hemiphyllodactylus* Bleeker, 1860 (Reptilia: Squamata) from Hunan Province, China. *Asian Herpetological Research*, **11**(3): 183−193.
Zhou KY, Liu YZ, Yang GP. 1981. Three new subspecies of *Hemiphyllodactylus yunnanensis* (Boulenger) from China (Lacertiformes: Gekkonidae). *Acta Zootaxonomica Sinica*, **6**(2): 202−209.
Zug GR. 2010. Speciation and dispersal in a low diversity taxon: the Slender geckos *Hemiphyllodactylus* (Reptilia, Gekkonidae). *Smithsonian Contributions to Zoology*, **631**: 1−70.